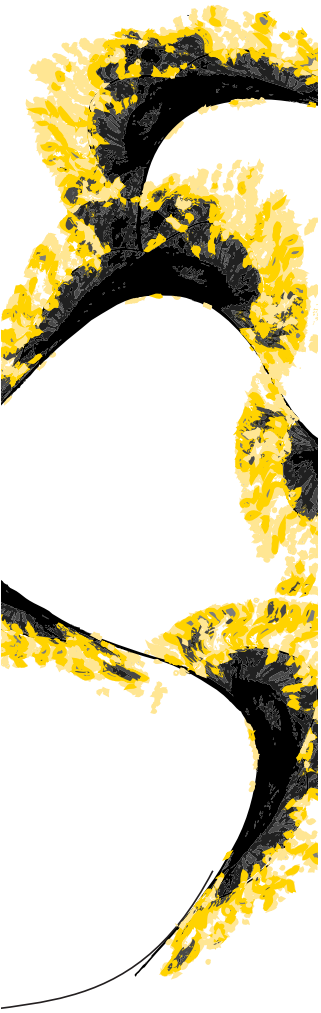

RAM ROBOTICS AND MECHATRONICS

COMPARING PROCESSING TECHNIQUES FOR REAL-TIME FORCE ESTIMATION FROM SEMG

T.J. (Tjeerd) Bakker

BSC ASSIGNMENT

Committee:
prof. dr. ir. G.J.M. Krijnen
ir. M. Schouten
prof. dr. ir. M. Sartori

July, 2022

032RaM2022
Robotics and Mechatronics
EEMCS
University of Twente
P.O. Box 217
7500 AE Enschede
The Netherlands

UNIVERSITY OF TWENTE. | TECHMED CENTRE UNIVERSITY OF TWENTE. | DIGITAL SOCIETY INSTITUTE

Abstract

Surface Electromyography (sEMG) is the technique of measuring the electrical activity that forms on the skin surface in in response to a muscle contraction. sEMG signals can be used to determine the status of muscles and the movement intention and is therefore commonly used as a control interface for robotic prosthesis or in the medical field to monitor muscle activity. To convert the measured surface potential into a usable signal, the data needs to be processed to filter out noise and determine the envelope. Even though a lot of research has been done into various processing techniques, a general overview comparing the differences in performance of these techniques is lacking. This report aims to give insight into the degree of effectiveness of pre-whitening, various filtering methods, and multiple envelope estimation techniques. The goal is to find a combination of methods that can accurately estimate exerted force from the sEMG signals in real-time. The filtering methods that are compared are a static filter (bandpass and notch filters), a Wiener filter, and an adaptive LMS filter. The envelope detection methods that are compared are a moving average filter, an infinite impulse response Butterworth low-pass filter, and a root-mean-square filter. Each method has been applied in a simulated environment to determine the optimal parameters, and every combination of pre-whitening, filtering, and envelope detection has also been applied on a measured sEMG sample. The resulting force estimates are subsequently compared to force measurements obtained using a calibrated load cell. The measurement results indicate that using adaptive filtering using the LMS algorithm combined with RMS envelope detection results in predicting the exerted force approximately half a second before it is measured. Whitening does not seem to improve the quality of force estimation and introduces consistent lag compared to non-whitened processing methods.

Keywords: sEMG, force estimation, signal processing

Contents

0.1 List of symbols . . . 1
0.2 List of medical terms . . . 1

1 Introduction **2**
1.1 Context . . . 2
1.2 Related work . . . 2
1.3 Research goal . . . 3
1.4 Conclusion . . . 4

2 Theory **5**
2.1 Force estimation from sEMG . . . 5
2.2 sEMG signal properties . . . 6
2.3 Filters . . . 7
2.3.1 Static filters, Wiener filter, Adaptive filters . . . 9
2.3.2 FIR vs IIR . . . 12
2.4 Pre-whitening . . . 13
2.5 Envelope detection . . . 15
2.5.1 Moving average . . . 16
2.5.2 IIR Low-pass filter . . . 16
2.5.3 Root Mean Square . . . 16
2.6 Standard sEMG signal processing . . . 18
2.7 Conclusion . . . 18

3 Simulation **19**
3.1 Pre-whitening . . . 19
3.1.1 Method . . . 19
3.1.2 Results . . . 19
3.2 Filtering . . . 19
3.2.1 Comparison metrics . . . 19
3.2.2 Method . . . 21
3.2.3 Results . . . 24
3.3 Envelope estimation . . . 25
3.3.1 Comparison metrics . . . 25
3.3.2 Method . . . 27
3.3.3 Results . . . 28
3.4 Force estimation . . . 30
3.5 Conclusion . . . 30

4 Measurements **32**

4.1 Experimental setup 32

4.2 Measurement data 33

4.3 Measurement processing result 35

4.4 Conclusion 42

5 Discussion and conclusion **43**

5.1 Discussion 43

5.2 Conclusion 44

5.3 Recommendations 44

A Appendix 1 **45**

Bibliography **49**

0.1 List of symbols

This table contains an overview of the symbols used in this work, their associated meanings, and their units.

Symbol	Definition	Unit
f	Frequency	Hertz (Hz)
f_{cut}	Cut-off frequency	Hertz (Hz)

Table 1: Symbol definitions

0.2 List of medical terms

A list of medical terms is given because the reader is expected to be an electrical engineer and not a medical student.

Term	Definition
Skeletal Muscles	Muscles that are used to control voluntary body movement
Flexor	A muscle that when contracted causes the angle between bones connecting to a joint to decrease (e.g. a Bicep)
Extensor	A muscle that when contracted causes the angle between bones connected to a joint to increase (e.g. a Tricep)
Antagonistic Muscles	A set of a flexor and extensor that have the ability to freely move a limb around a joint
Isometric Contraction	A muscle contraction that does not result in a change of joint angle (e.g. the joint is blocked or antagonistic muscles contract simultaneously)
Isotonic Contraction	A contraction of antagonistic muscles that causes the angle of the joint to change

Table 2: Medical terms

1 Introduction

1.1 Context

Electromyography (EMG) is the technique of measuring the electrical activity that forms in a muscle in response to a nerve stimulating the muscle fibers [1] [2]. EMG is a popular method of measuring a person's intent to contract a muscle as it measures the muscle activation rather than the muscle contraction [3] [4]. This means that it can still be used in scenarios where muscles can not respond accurately to nerve stimulation due to for example muscular dystrophy [5]. As a result, EMG is a good way of creating a control interface for exo-aids in various scenarios. Additionally, the amplitude of the EMG signal has a roughly linear relation with the force produced by the muscles in specific circumstances [6] and is therefore suitable for human machine interfaces [7].

The electrical activity of a muscle can either be measured by probing the inside of a muscle (called intramuscular EMG or iEMG), or by measuring the electrical potential on the surface of the skin (called surface EMG or sEMG). iEMG has a high selectivity for individual motor neuron units which is desirable for a precise control interface registering multiple degree of freedoms [8], but has as a downside that it is an invasive and difficult procedure [9]. sEMG is a non-invasive method of measuring requiring only sticking electrodes on the skin but this method can only measure the combined electrical activity of many muscle fibers resulting in a noisy and imprecise signal [10].

During the last two decades research has attempted to gather more accurate sEMG readings by increasing the number of electrodes on a muscle with a technique called high-density sEMG [11]. This technique has allowed the measuring of spatial muscle activation in addition to time domain muscle activation. By measuring the muscle activation of a single muscle at multiple points in space it is theoretically possible to determine the behaviour of individual motor units [12].

However, this increased accuracy comes with a catch: each electrode outputs a single data stream that needs to be processed. Adding more electrodes means requiring more amplifier channels and smaller electrodes with higher contact impedance [13], both of which results in more expensive amplifiers. Additionally, having to process more data requires a faster signal processing chain as the introduction of additional processing delay may prevent successful control of exo-aids [14].

This project aims to give an overview of the effectiveness of various EMG processing techniques. The effect of whitening the input signal, different filtering techniques, and different envelope detection techniques are discussed, with the overarching goal of performing accurate force estimation from sEMG signals.

1.2 Related work

There are a number of works on applying different filtering techniques in the medical field. Some interesting papers that closely relate to this assignment are discussed.

An example that shows the effectiveness of adaptive filters for real-time signal processing is the work by M. Hanine et al. [15] which covers the removal of an EMG signal from an electrocardiogram (ECG, electrical activity around the heart) signal. This is notable because the signal spectra of EMG and ECG overlap to a large extend and are therefore notoriously hard to remove using static filters. Furthermore it is mentioned in [16] that adaptive filters might be the most suitable type of filters for estimating force from sEMG signals.

The performance of adaptive filters and Wiener filters for noise cancellation in real-time environments in general has been tested in the works of G. Yadav et al [17]. This report provides a solid groundwork for an intuitive understanding of wiener filters and adaptive filters which are used in this project.

A bold but promising implementation of Wiener filter in sEMG is presented in the work of J. Liu et al [18]. This paper presents the problem of voluntary EMG signals being contaminated by spontaneous unwanted motor activity from paretic muscles in for example stroke or spinal cord injury patients. The research uses an 'a priori' SNR (deduced from theory, not measurements) to filter the EMG signal from the involuntary muscle contractions.

A common technique of improving signal integrity through pre-processing is 'whitening'. Whitening decorrelates the sEMG signal to yield improved signal accuracy [19]. Whitening can primarily be used for high-amplitude EMG signals and has trouble retaining effectiveness on low amplitude signals. This problem has been attempted to solve by creating adaptive whitening filter which shows promising results when applied to low EMG amplitude signals as shown in the work of E. Clancy and K. Farry [20].

An important paper in the field of EMG signals is the work by N. Hogan and R.W. Mann [21]. This research aims to provide a fully mathematical solution for an optimal myoelectric signal processor, and to do so a phenomenological mathematical model of myoelectric activity is presented. In other words: This paper uses biology, physics and statistics to create a framework that allows predicting the EMG signal that would form from muscle activity.

There are several papers related to signal processing of sEMG signals. One outstanding example is the work by M.Z. Jamal et al [7], where it is shown that adaptive filters are an effective solution to EMG signal processing. The paper presents the instrumentation scheme of a dry-electrode sEMG measurement setup and explains a method of creating real-time adaptive finite impulse response (FIR) filters. In essence this is close to a part of this research, but the aim of this research project is aimed at *comparing* the performance between filtering methods rather than the creation of a specific one.

Lastly it should be mentioned that static and adaptive filters are only a subset of the available tools for sEMG signal processing. An emerging topic in this field is the use of machine learning methods for signal analysis. Applying machine learning could allow for fast, efficient, and effective signal processing, with the downside of unpredictable behaviour in certain situations. Where static filters and adaptive filters exhibit deterministic behaviour (which is difficult to confirm in the case of real-time adaptive filters), machine learning methods can be somewhat 'hit or miss'. [22, 23]. It has been found that machine learning models at times violate their original expectations after deployment. The main reason for this is that the models often contain varying and unknown failure modes that are only revealed after deployment due to the complexity of the model and the lack of understanding of internal systems (black-box behaviour) [24].

1.3 Research goal

Even though a significant amount of research has been done into the digital processing of sEMG signals, an overview comparing different techniques is lacking. This report aims to give an overview of pre-whitening, different filtering techniques, and multiple envelope detection techniques. The goal of this project is to explore the difference in performance of different sEMG signal processing chains when applied to sEMG signals for real-time force estimation. In Figure 1.1 a high-level overview of the signal processing chain is presented.

These research efforts are driven by the research question below.

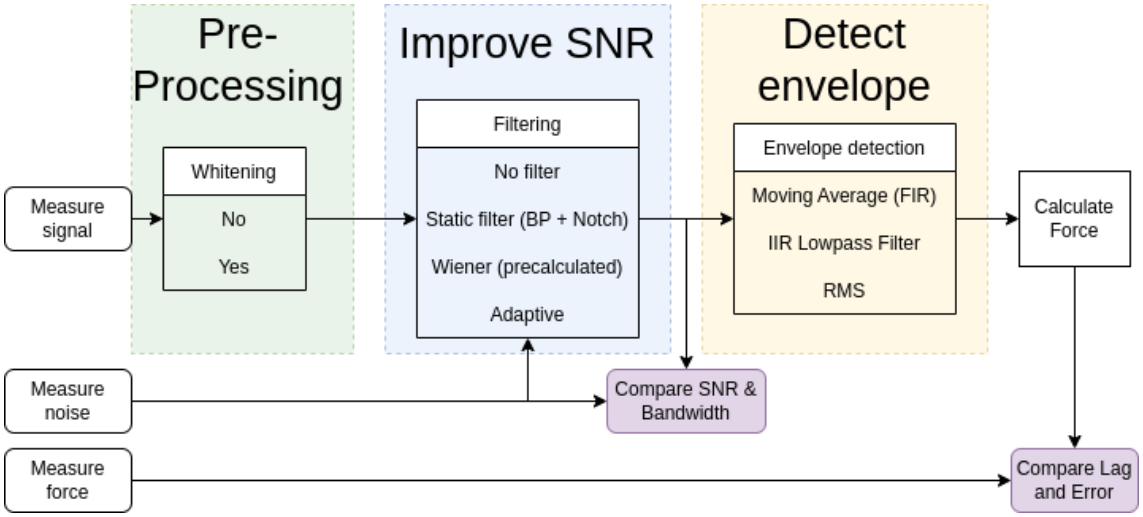

Figure 1.1: High-level overview of the signal processing chain

What is the best combination of whitening, filtering, and envelope detection to estimate force from sEMG in real-time?

This report consists of three main sections:

- In the theory section the background of each option in each processing step (whitening, filtering, and envelope detection) is explained
- In the simulation section it is shown how different parameters influence the behaviour of each option in a simulated environment
- In the measurements section it is shown how all possible combinations from each processing step perform on a measured sEMG signal to find the optimal sEMG processing chain

The observations that were made from the simulations and measurements are further discussed in the discussion section.

1.4 Conclusion

Surface EMG is a popular tool for determining muscle activation and user intent and can be used as a human-machine interface. There exist many different methods to extract useful information from sEMG signals, but a general overview of different techniques and how they compare to each other is lacking. The topics covered in this report are (pre-) whitening, filtering using static filters, Wiener filter, and adaptive LMS filter, and envelope detection using moving average, root mean square, and infinite impulse response low-pass filters.

2 Theory

The required background theory will be presented in a top-down approach. For someone experienced in the field of sEMG and signal processing some portions can be perceived as ubiquitous but it is done to make this paper more accessible for readers from different fields.

2.1 Force estimation from sEMG

When moving a limb the most intuitive way of describing it is a change in position, moving your hand from A to B. However, a more objective way of describing this movement is in terms of forces applied on a mass [25–27]:

- The brain makes decision to move a limb and sends a signal through motor neurons
- The synaptic input received from the motor neuron results in contraction of the muscles
- This (simply put) causes a force to be applied on a mass, or a torque around a pivot point
- This force results in an acceleration in a certain direction
- This acceleration is maintained for a certain period of time
- The entire process is repeated for deceleration using visual, kinesthetic, proprioceptive and tactile sensory signals [4]
- Your limb has arrived at a new location.

Understanding this reasoning of moving a limb in terms of forces being applied by contracting muscles is vital because it forms the basis for recognizing a user's intent. EMG can be used to measure the intensity of muscle activation which indicates the amount of contraction [4]. By measuring the amount of contraction of two antagonistic muscles it is possible to calculate the amount of force applied in a certain direction. Even if the limb is replaced by a prosthesis this idea of forces moving a mass will still apply, and thus EMG can be used as a human-machine interface.

So to summarize the basic concept of force estimation:

- Movement of a limb is the result of a net force acting on that limb
- This net force is the result of certain muscles contracting stronger than other muscles
- The contraction of these muscles follows from muscle activation
- Muscle activation can be measured using EMG
- EMG can be used to estimate limb movement

Figure 2.1 illustrates the anatomy of a muscle. Large skeletal muscles such as the biceps consists of hundreds of thousands of small muscle fibers. These muscle fibers are divided into groups called motor units, and each motor unit is connected to a motor neuron which is a special type of very long brain cell that runs through the spinal cord. A contraction of a skeletal muscle is the result of many muscle fibers contracting individually and repeatedly [26]. The contraction of these muscle fibers is the result of muscle activation which in turn is the result of an action potential caused by the motor neuron. The activation of the muscle fibre is a small yet measurable voltage. When measuring the surface EMG of an activating skeletal muscle the result is the aggregate of the small voltages from all activating muscle fibers. This manifests

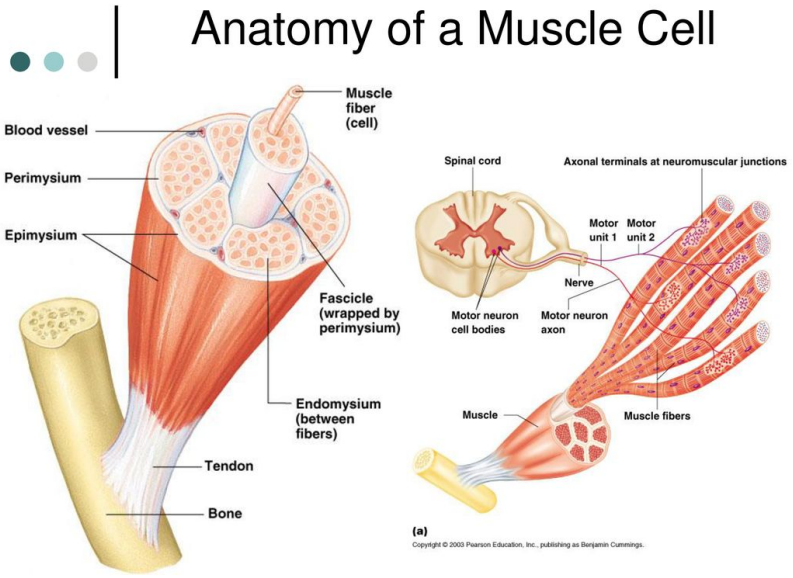

Figure 2.1: Anatomy of a muscle [26].

itself into a signal resembling white noise where the amplitude of the noise correlates to the number of activated muscle fibers and thus to the amount of contraction the skeletal muscle will experiences [21]. An illustration of the form of the measured sEMG is shown in Figure 2.2 where a maximum voluntary contraction (MVC) is measured from a biceps.

2.2 sEMG signal properties

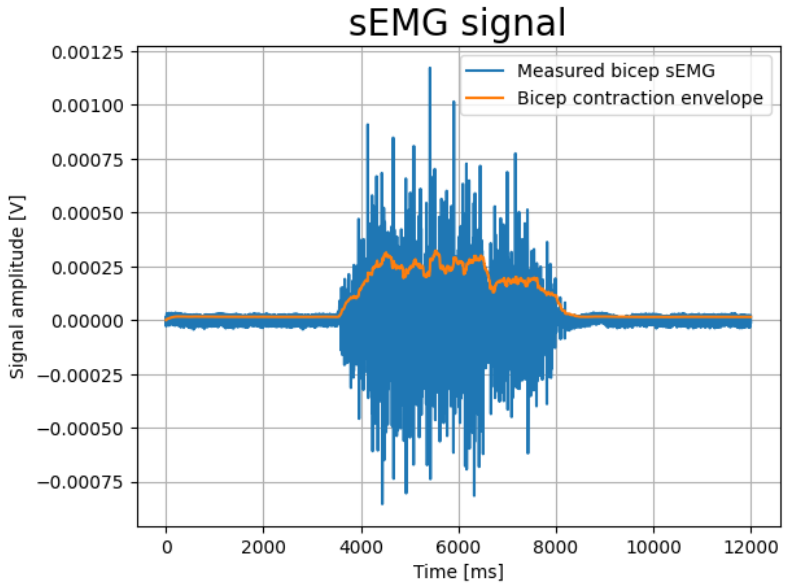

Figure 2.2: sEMG signal measured from bicep during contraction

To summarize: to determine the degree of activation of a skeletal muscle we simply need to determine the amplitude of the noise at the surface of the muscle.

From this point onward 'noise' will refer to the generated by muscle contraction as 'the signal'. the reason for this is that noise is usually unwanted, but the signal caused by muscle contraction is the opposite of unwanted: It precisely what sEMG is trying to measure!

Unfortunately, when measuring sEMG signals it is impossible to measure solely the signal generated by muscle contraction. The signal may be contaminated by other signals coming from the surrounding environment or from the amplifier used to amplify the measured signal. So in reality we are measuring a combination of our desired signal from muscle contraction, and the undesired noise from the environment and amplifier. An illustration of the frequency content of the signal and noise is shown in Figure 2.3. Note how the noise has large peaks at 50 Hz and multiples of 50 Hz; This is the noise generated by power lines nearby.

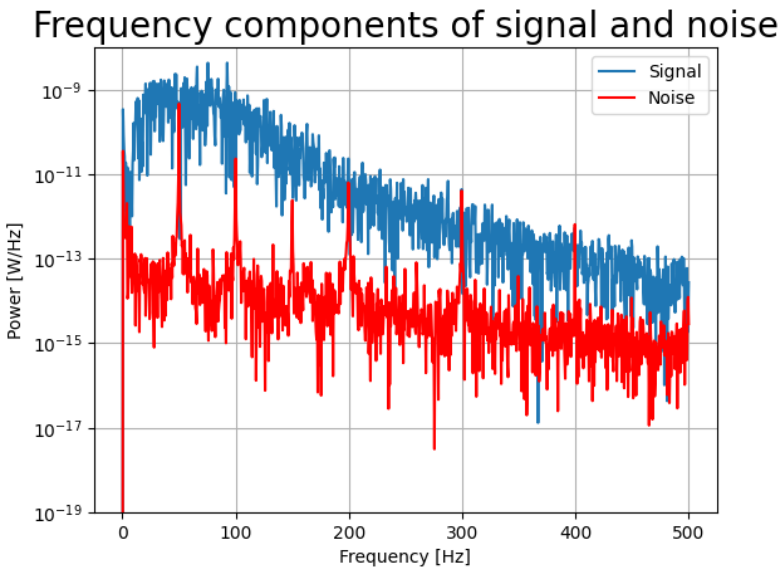

Figure 2.3: Frequency components of signal and noise in an sEMG signal. Noise is taken to be 0-2s and Signal is taken to be 5-7s in 2.2

The ratio between how much of the measured signal is actual desired signal and how much is undesired noise is called the Signal to Noise Ratio (SNR) and is defined as the average signal power divided by the average noise power and can be seen in Equation 2.1 [28]. Intuitively one might think that force can be more accurately estimated from sEMG signals with a high SNR, this assumption will be tested in this report. SNR can be increased by removing noise from a noisy signal which can be done by a selection of tools called filters.

$$\text{SNR} = \frac{\text{Signal power}}{\text{Noise power}} \tag{2.1}$$

2.3 Filters

Filters are a tool that can be used to remove something unwanted (noise) that is mixed with something wanted (signal). In signal processing filtering is achieved by decomposing a measured signal into repeating patterns and subsequently deciding which patterns should be retained and which patterns should be removed. Figure 2.4 displays how a time-domain signal can be represented in the frequency domain to display information about which frequencies are present in the signal.

A digital filter consists of a set of values called the filter coefficients. The input (measurements) is multiplied with the filter coefficients to create the output. That is, the latest measurement

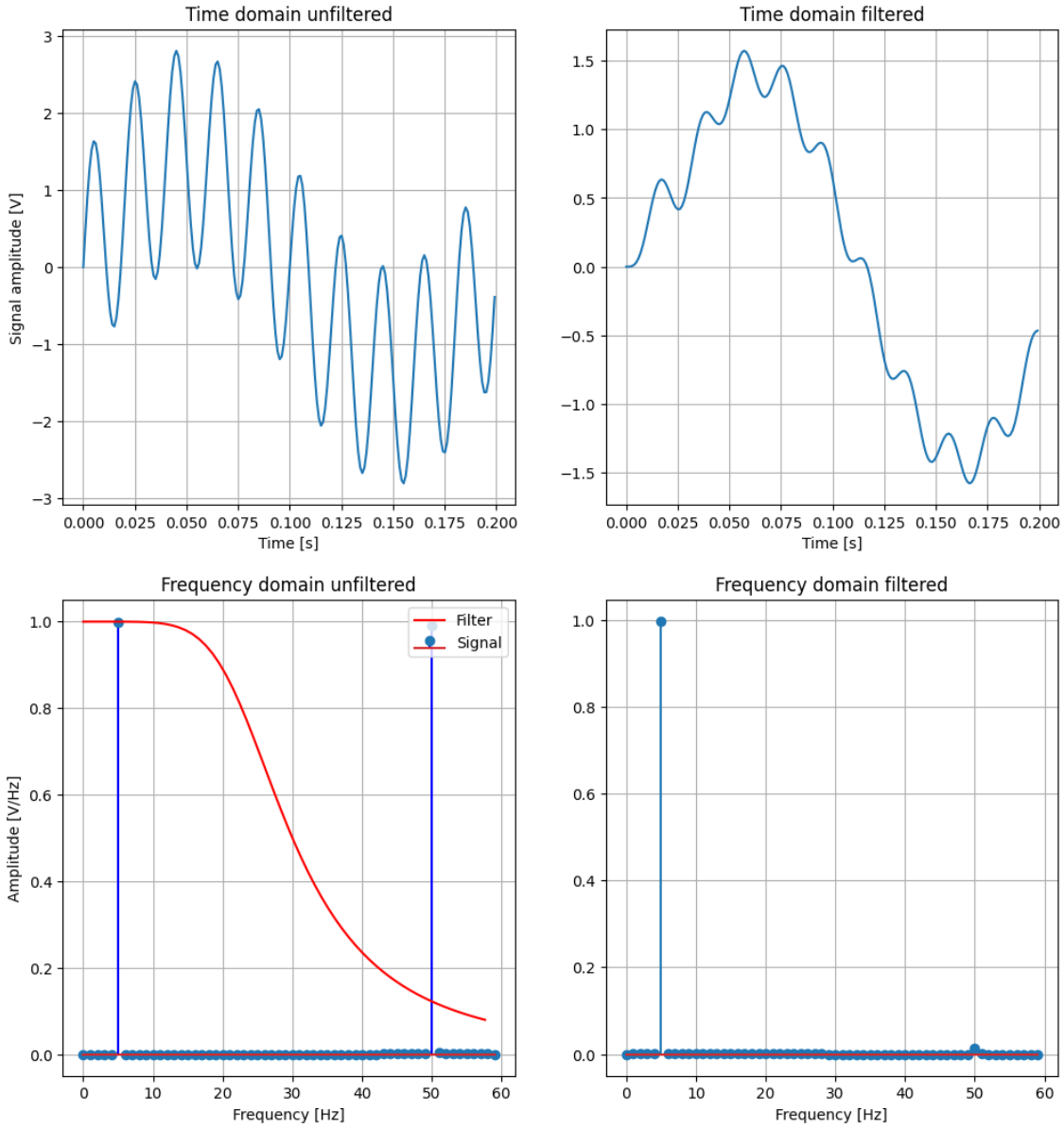

Figure 2.4: Filtering a signal. In the top-left figure there is a low-frequency signal polluted by a 50Hz signal. The frequency plot in the bottom-left shows these frequencies. By applying the low-pass filter as displayed in the bottom-left it is possible to filter out the higher 50 Hz frequency. The resulting filtered signal can be seen in the top-right, showing that there is still a little bit of noise left. This is also visible in the bottom right showing the frequency contents of the signal after filtering

is multiplied with the first filter coefficient, the previous measurement is multiplied with the second filter coefficient, and so on. This can also be interpreted as multiplying each filter coefficients with a delayed input sample. Figure 2.5 shows the working and standard notation of a digital filter. By carefully choosing the number and value of filter coefficients it is possible to attenuate specific frequencies while not influencing other frequencies such as the effect shown in 2.4.

Analog signals and filters are conventionally presented as a continuous function of time (e.g. $x(t)$). Digital signals and filters are discrete rather than continuous, and are conventionally presented as a function of samples (e.g. $x(n)$). The variable n describes the n'th sample of

the signal. Converting a continuous signal to a discrete signal is done through the process of sampling the continuous signal at equidistant points in time: $s(n) = s(n * \Delta t)$ [29].

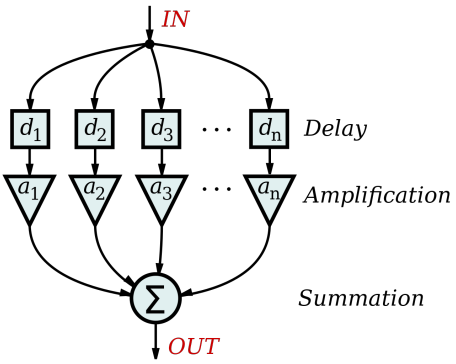

Figure 2.5: The functioning of a digital filter. The filter coefficient at index i is multiplied by the input that is delayed i samples [30]

2.3.1 Static filters, Wiener filter, Adaptive filters

The main difference between the different presented filter types is the way of calculating the filter coefficients. If a filter is static (e.g. high-pass, low-pass, band-pass, or band-stop) it simply means that the number of filter coefficients and the values of the filter coefficients are predetermined. These filters are very popular due to their simplicity in terms of finding the value of the filter coefficients.

A Wiener filter aims to produce an estimate of a target process by linear time-invariant filtering of a noisy signal using knowledge of the spectrum of the stationary noise and target process assuming additive noise [31, 32]. Figure 2.6 shows the use of a Wiener filter. It is assumed that the noise component $v(n)$ is correlated to the noise component in the input signal in input $d(n)$ and uncorrelated to the desired signal $s(n)$. The Wiener filter coefficients aim to minimize the correlated signals, leaving only the desired signal as the 'error'. It is the optimal solution in terms of mean square error to statically filtering additive noise from a signal. The filter can either be constructed from the cross-correlation between an input sample and a noise sample, and the auto-correlation of the noise sample, or directly from the frequency contents of the signal+noise and noise signals as seen in Equation 2.2.

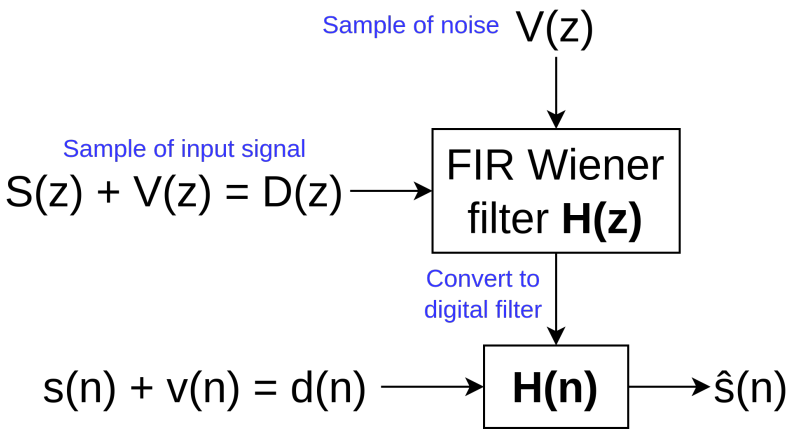

Figure 2.6: Diagram that illustrates the functioning of a Wiener filter. $s(n)$ is the desired signal, $v(n)$ is the additive noise, and $d(n)$ is the combination of desired signal and noise [33]

In sEMG, the signal+noise is measured at the point of muscle contraction while the noise can be measured separately from a different body part that does not experience contraction. This separately measured noise has similar frequency characteristics as the noise included in the signal+noise as it experiences the same amplifier noise and environment noise. The resulting frequency domain definition of the optimal Wiener filter is defined in Equation 2.2 [34]. $D(z)$ reflects the frequency contents of signal+noise (input signal), $S(z)$ reflects the frequency contents of the signal, and $V(z)$ reflects the frequency contents of the noise.

$$H_{\text{opt}}(z) = \frac{S(z)}{S(z)+V(z)} = \frac{D(z)-V(z)}{D(z)} \tag{2.2}$$

Assuming that the calculated Wiener filter approximates the optimal Wiener filter, multiplying the filter (in frequency domain) with the signal+noise input will result in an approximation of the signal as seen below.

$$\begin{aligned} \hat{S}(z) &= \hat{H}_{\text{opt}}(z) \cdot (S(z)+V(z)) && (2.3)\\ &= \frac{\hat{S}(z)}{\hat{S}(z)+\hat{V}(z)} \cdot (S(z)+V(z)) && (2.4)\\ &\approx S(z) && (2.5) \end{aligned}$$

The Wiener filter requires both the signal and the noise to be stationary, i.e. the spectral density does not change over time, and results in a linear time-invariant filter [35] [36]. If the signal and noise were not stationary then the approximated frequency spectrum of signal+noise is not the same as the actual frequency spectrum of signal+noise which means they no longer cancel out in Equation 2.4 and Equation 2.5 no longer holds. As an example a Wiener filter was made from the signal as seen in Figure 2.2. The time span from 0 s to 2 s is taken as the 'noise', and the time span from 5 s to 7 s is taken to be signal+noise. From these a Wiener filter is constructed and can be seen in Figure 2.7.

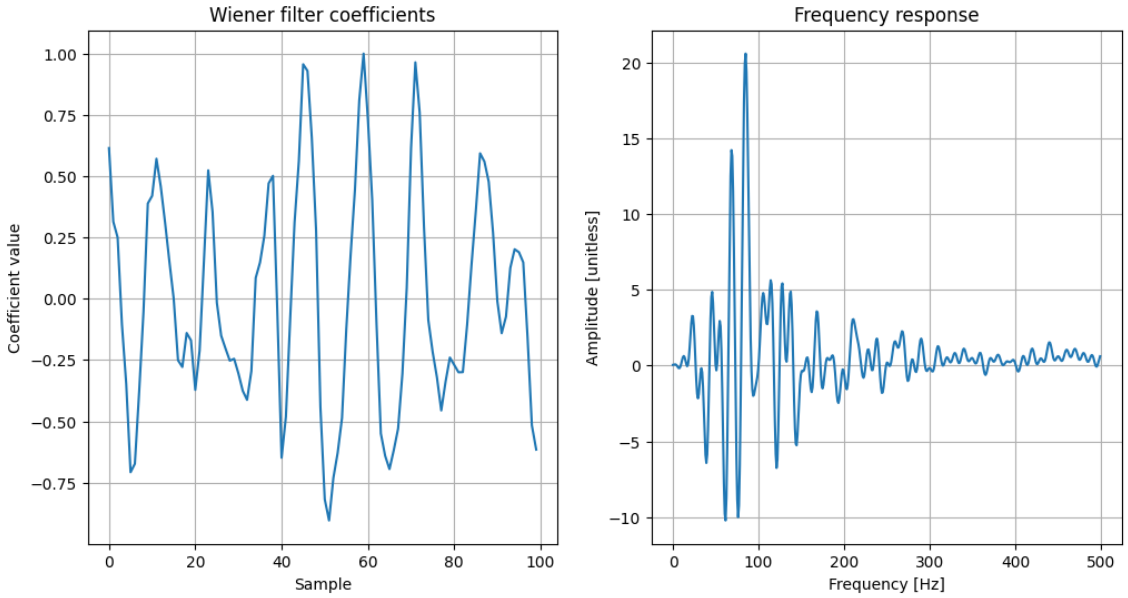

Figure 2.7: Filter coefficients and frequency responses of a Wiener filter

Adaptive filters are a class of filters where the filter coefficients are adjusted over time to attempt to find an optimal solution even without knowing the spectral properties of the signal

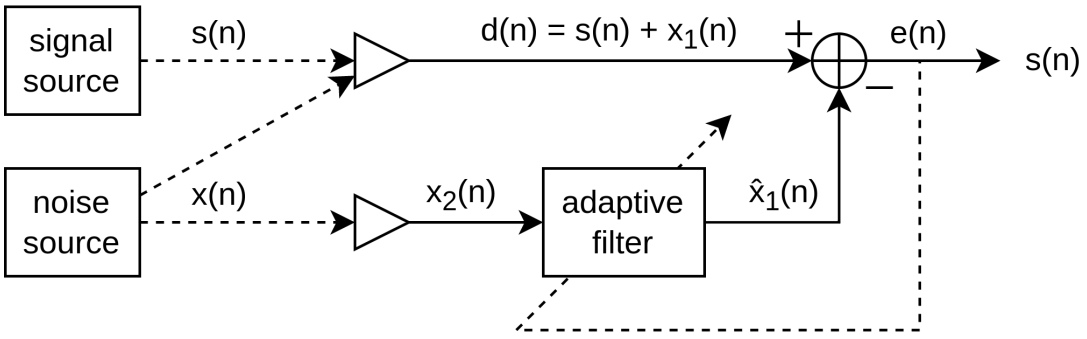

Figure 2.8: Block diagram of an adaptive filter [37]

beforehand [38]. Adaptive filters adjust the filter coefficients by decreasing the error that remains after applying the filter. A diagram describing this process can be found in Figure 2.8. One type of adaptive filter is the Least Mean Squares (LMS) algorithm. Where a Wiener filter finds an optimal solution by using cross-correlation and auto-correlation, the adaptive LMS algorithm converges to the optimal solution (i.e. the solution found by the Wiener filter given complete knowledge of the spectral domain) using gradient descent. Filter coefficients will never reach w_{opt} but instead oscillate around it. The mathematical definition for calculating the filter coefficients is given, derived from the work of J. Orfanidis [37, Ch. 7.3] and lectures by S. Safapourhajari [39]. Again it is assumed that there is an input signal ($d(n)$) consisting of a desired signal ($s(n) = e(n)$) and additive noise ($x(n)$), as well as a separate measure of the noise that is correlated with the noise in the input signal but uncorrelated with the desired signal. The desired signal $s(n)$ is also called the error $e(n)$ since it is the remainder after removing the noise from the signal+noise, as well as the fact that this is convention [37].

The cost function for adjusting the adaptive filter as seen in figure 2.8 coefficients is taken to be the Mean Square Error J (MSE):

$$J(w) = E(e^2(n)) = E[(d(n) - wx(n))^2)] \tag{2.6}$$

To calculate the expected value of the square of the error we would normally need statistics over a large block of data. An approximation of the expected value can be made by using a smaller set of data. This can be done by taking the current samples as the estimates of the mean

$$E(e^2(n)) \sim e^2(n) \tag{2.7}$$

Since the error $e(n)$ equals $d(n) - wx(n)$ this can be filled into the equation

$$E\left((d(n) - wx(n))^2\right) \sim (d(n) - wx(n))^2 \tag{2.8}$$

To find w that minimizes the MSE we can take the derivative of MSE with respect to w for every sample n

$$\frac{\partial J}{\partial w} = 2\,(d(n) - wx(n))\,\frac{\partial\,(d(n) - wx(n))}{\partial w} = -2e(n)x(n) \tag{2.9}$$

This results in the following weight-adjusting algorithm

$$w(n+1) = w(n) - \mu \frac{\partial J}{\partial w}\bigg|_{\text{w(n)}} \tag{2.10}$$

$$= w(n) + 2\mu e(n)x(n) \tag{2.11}$$

This algorithm is implemented by performing the following steps.

1. The estimated value for signal+noise is computed from the filter and noise

$$\hat{x}_n = w(n) \cdot y(n) \tag{2.12}$$

2. The error is calculated by taking the difference between the expected signal+noise value and the measured signal+noise value.

$$e(n) = x(n) - \hat{x}_n \tag{2.13}$$

3. The coefficients are calculated for the next iteration

$$w(n+1) = w(n) + 2\mu e(n)x(n) \tag{2.14}$$

The steps in equations 2.12-2.14 are repeated for every next sample.

In the presented equations a constant μ is present; this is called the convergence coefficient. Determining the value of the convergence coefficient μ is a double-edged sword. On the one hand it determines how fast the gradient descent is traversed, and thus how fast the filter coefficients converge to the optimal filter coefficients. Ideally this happens as fast as possible, and thus the convergence coefficient must be as large as possible. On the other hand it was previously mentioned that the filter coefficients will never reach the optimal filter coefficients but instead oscillate around this value. The convergence coefficient also determines how large this oscillatory behaviour is, and thus to achieve an accurate estimation of the optimal filter the convergence factor should be as small as possible.

A problem presented by the basic LMS algorithm is that scaling the input also results in scaling the error term calculated in Equation 2.13. This makes it difficult (if not impossible) to find a convergence factor that functions across a wide range of possible scaled inputs. A solution to this problem is found in the work of Haykin [40] in the form of the Normalized LMS filter. This normalizes the power of the input signal before multiplying the input with the error and convergence factor. This is done by dividing the input signal with the dot product of the input signal with itself. It turns Equation 2.14 into Equation 2.15 [40]. It should be noted that since the filter coefficients are updated over time, the final result of the coefficients are only the approximation of the optimal coefficients that correspond to the last part of the signal. This holds true especially for non-stationary signals. Purely for completeness the final result of an LMS filter has been given in Figure 2.9.

$$w(n+1) = w(n) + 2\mu e(n)\frac{x(n)}{x(n) \cdot x(n)} \tag{2.15}$$

Common applications of adaptive filters include speech recognition, echo cancellation, and headphones employing active noise cancellation [17, 41].

2.3.2 FIR vs IIR

Another subdivision within filter design is concerned with the type of possible responses to a specific input (impulse) and whether or not this can go to infinity.

The previously discussed filters were all described as Finite Impulse Response (FIR) filters. This means that the output is the result of multiplying the filter coefficients with the input. This type of filter is always stable and the output can never go to infinity as long as the input does not go to infinity.

An Infinite Impulse Response filter calculates the output using two sets of filter coefficients. The first set of filter coefficients is used to multiply the input with just like an FIR filter, but the second set of filter coefficients is used to multiply the previous *outputs* with. This means that

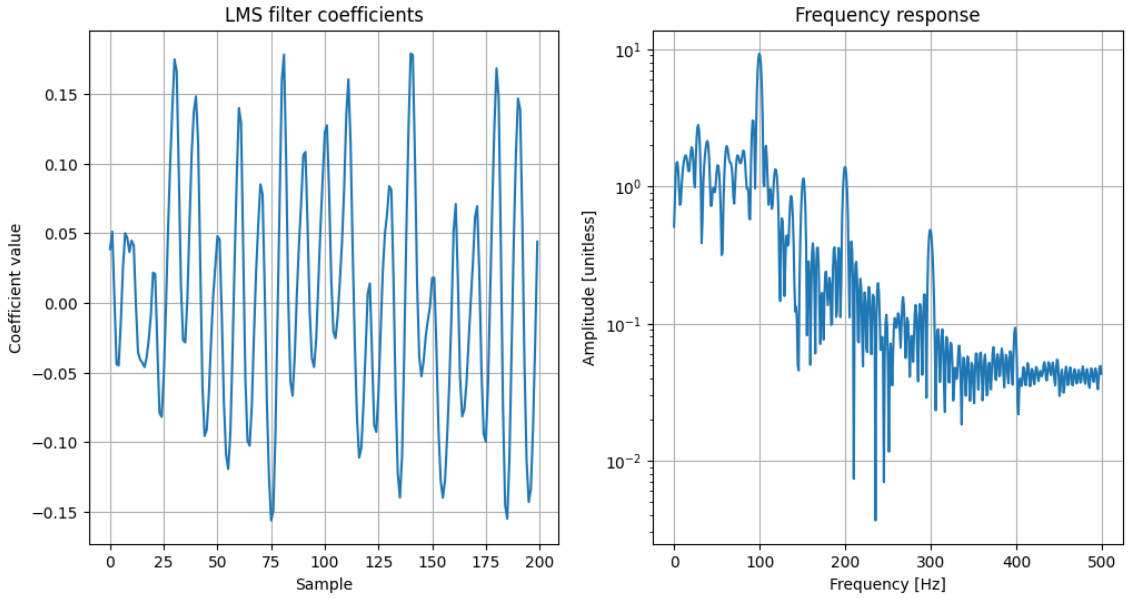

Figure 2.9: Filter coefficients and frequency response of an adaptive LMS filter

there is now a feedback loop in the system, and a system with feedback can become unstable. Unstable in this case means that there is a possibility of positive feedback loops where increasing output values result in future output values also increasing, eventually going to infinity. Even though this feedback and possible instability may sound like a downside, it also results in shorter filter length and thus fewer computations required per filter operation. This could especially turn out to be beneficial in low memory and low compute power environments like in prostheses [42].

Both static and adaptive filters can be implemented as either FIR or IIR filters. An adaptive IIR filter offers the potential to meet desired performance levels with much less computational complexity. However, the possibility for the system to become unstable combined with the fact that filter coefficients are adjusted automatically leads to a high-risk high-reward scenario due to a loss of control and hard to predict behaviour [43].

2.4 Pre-whitening

During literature research it was noticed that it was not uncommon in literature to mention something along the lines of "including a temporal whitening filter [...] improves the performance of the amplitude estimate" [19,20,45]. However, an intuitive explanation of *why* whitening works was consistently lacking. So to understand the reasoning behind whitening we need to take a short detour to the world of computer science and information theory.

Back in 1948 a mathematician, electrical engineer, and cryptographer named C.E. Shannon published a pioneering paper that formed the basis of information theory [46]. In this paper it is shown that repetition does not carry information, and that the maximum information transfer occurs when a signal is truly random. Imagine a signal with only a single frequency component. After measuring a few samples of the signal the conclusion is drawn that this is a 50 Hz signal. Since it is possible to predict the value of every future measurement of the signal after drawing this conclusion it becomes unnecessary to continue measuring the signal because it will not give any new information. A repeating pattern is predictable, and predictable events carry no information.

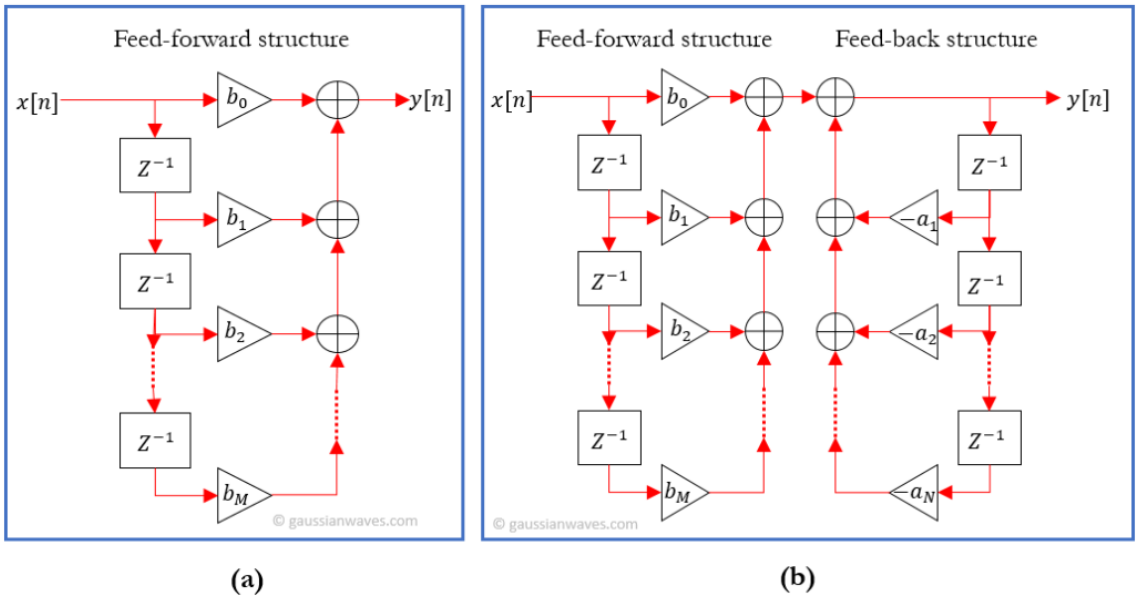

Figure 2.10: A diagram displaying the difference between Finite impulse response filters, only using previous input, and Infinite impulse response filters, using previous inputs and previous outputs resulting in a feedback loop [44]

The polar opposite of a signal containing a single frequency (and therefore predictable and carries little information) is a signal that contains all frequencies an equal amount. This is called a white noise signal and carries the maximum amount of information because there exists no repetition and therefore every sample carries new, unpredictable information.

Between the existence of a signal containing a single frequency, and a signal containing all frequencies (white noise), all other signals exist and have certain frequencies that are more 'present' than other frequencies. These signals have different degrees of predictability (and thus information density), and the degree of predictability is determined by how closely the frequency content resembles white noise.

Whitening is a filtering technique that tries to equalize the presence of frequency components in a signal to approximate white noise and thus increase information density. It reduces the random error and yields a larger dynamic range because the small frequency components that contribute to the 'randomness' of the signal but not so much to the value of the measurement sample become more present [47, Ch. 5.4.9] [45]. The serial correlation of the signal is decreased by reducing the presence of 'predictable' signals, which increases the randomness and thus information density [48].

This previous information manifests itself in sEMG signal processing by the fact that the measured sEMG signal is not white. Some frequency components are much more present than others, but all frequencies equally contribute to the indication of muscle contraction. To get a more accurate indication of muscle contraction the signal should be whitened to increase the information of each sample.

Whitening in real-time is achieved through a digital filter with a frequency response that when multiplied with the sEMG signal frequency spectrum yields a white noise spectrum.

To summarize: Whitening reduces the power of repeating frequencies and increase the power of random frequencies in the signal. An example is given in Figure 2.11.

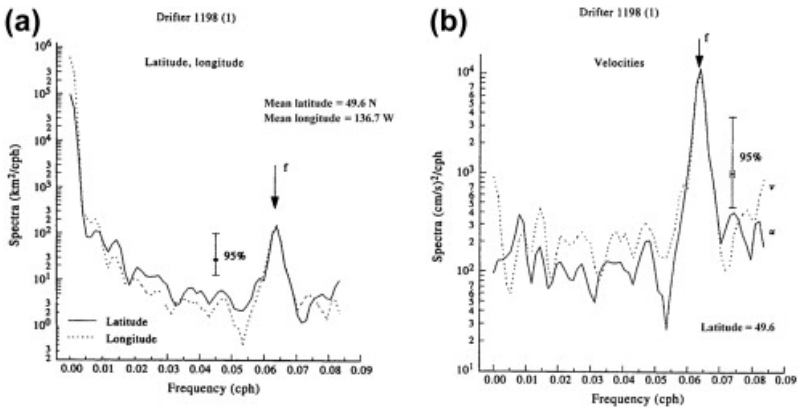

Figure 2.11: An example of whitening a signal. The indicated peak contains the 'random' signal of interest. By whitening the powerful lower frequencies it is possible to give the information-carrying peak more presence on the signal [47]. The focus with this figure should lie with the change in shape of the frequency spectrum, the actual represented data is irrelevant.

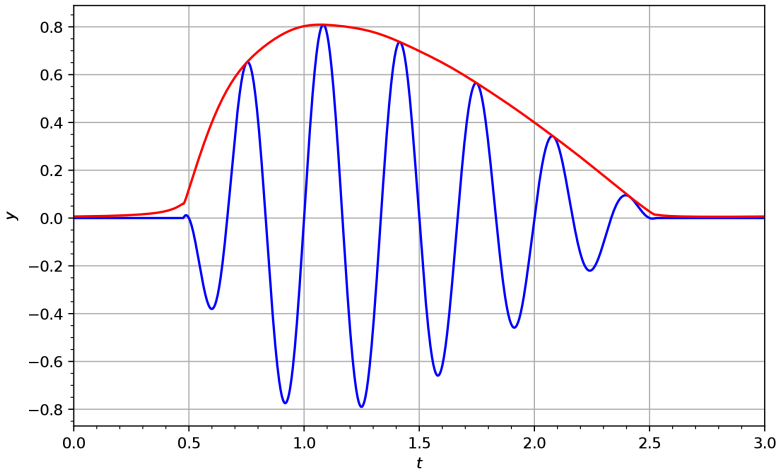

Figure 2.12: Illustrating envelope detection of an analytical signal [49]

2.5 Envelope detection

The relation between the amplitude of a measured sEMG signal, the degree of contraction of a skeletal muscle and the exerted force is very complicated. However, the relationship between force and EMG amplitude during isometric contractions is usually linear or close to linear [6] [7]. This is the reason that in this report it is assumed that there exists a linear relation between force and sEMG signals.

Since the raw EMG signal consists of stochastic and unpredictable noise it is difficult to draw conclusions about the degree of muscle contraction when solely looking at individual samples [50]. By drawing an outline of the peaks of the signal a much more informative picture can be drawn. This is called an envelope and an illustration of this process can be found in Figure 2.12. In the case of more random sEMG signals it is preferred to perform full wave rectification on the signal before calculating the envelope so that all of the signal energy is taken into account [50]. Applying this concept to an sEMG signal is illustrated in Figure 2.13.

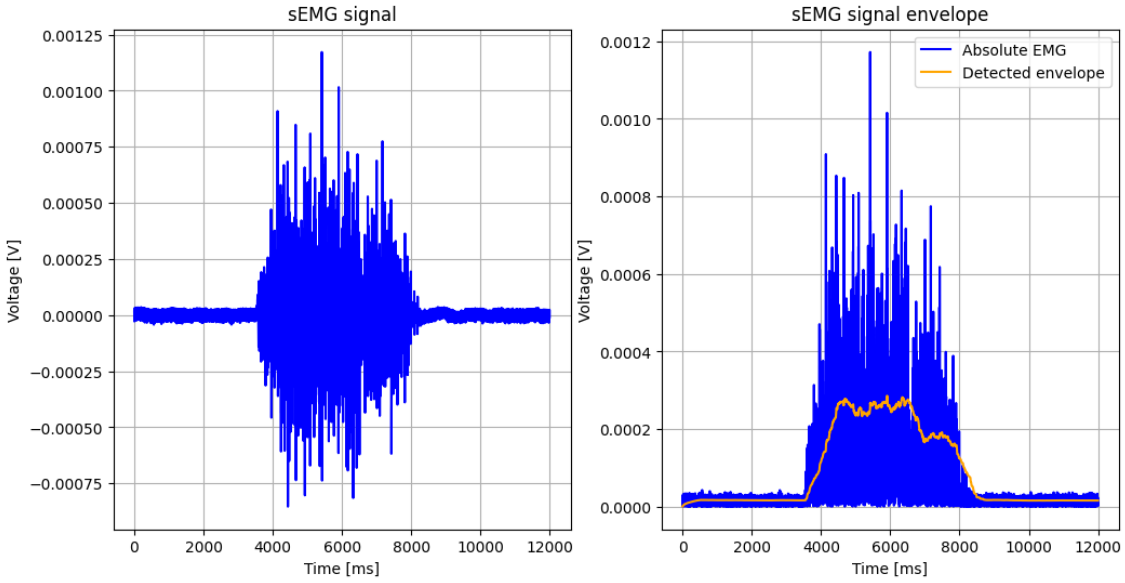

Figure 2.13: On the left a time-domain sEMG signal. On the right an example of envelope estimation is presented. By taking the absolute value of the sEMG signal on the left and calculating the envelope it is possible to make an estimation of muscle contraction. The next step would be force estimation but this requires two antagonistic muscles. This is discussed more in-depth in section 3.4

Computationally envelope detection can be achieved in a number of different methods where "speed", or how much the detected envelope lags behind the true signal envelope, is traded against accuracy or noisiness [51].

2.5.1 Moving average

The moving average filter used in this report is a special type of FIR filter with coefficients that all have the value of $\frac{1}{n}$ where n is the number of samples over which the average is taken. Thus the value of every smoothed sample is calculated to be the average of the previous n samples. The upside of a moving average filter is that it introduces no phase distortion [52], is very simple to implement, and requires only additions to apply which is much faster than multiplication [53]. An illustration of the phase shift of a moving average filter is shown in Figure 2.14. An intuitive downside of a moving average filter is that its output lags behind the signal: a change in a static signal level is only properly reflected after n samples. The sEMG signal must also be rectified before this method can be applied because EMG signal is of stochastic nature with zero mean [54].

2.5.2 IIR Low-pass filter

A low-pass filter such as a Butterworth or Chebyshev can be used to determine the envelope of a rectified signal in a more 'responsive' (less lag) method compared to a moving average filter. The downside of this filter is that it introduces phase shift (as can be seen in Figure 2.15) unless applied in forward and backward direction [54] which is not possible in real-time signals without introducing a static delay of a number of samples that equals the number of filter coefficients.

2.5.3 Root Mean Square

The Root Mean Square (RMS) of a signal is the square root of average power of a signal for a given period of time, a definition is given in Equation 2.16. A useful property of RMS is that when it is applied to a signal with Gaussian distribution the RMS amplitude of the source is the

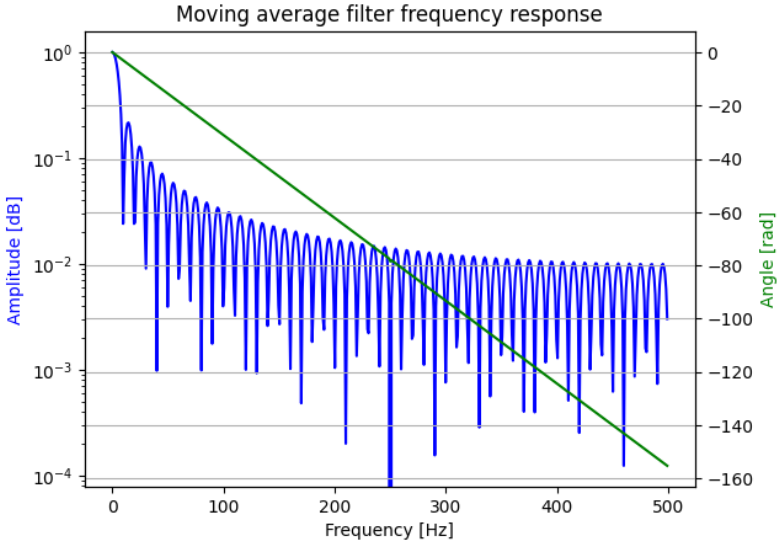

Figure 2.14: Frequency response of a moving average filter. This particular filter consists of 100 coefficients all equal to 0.01. Notice how the filter has linear phase which indicates that there is no phase distortion due to the time delay of frequencies relative to another [52]

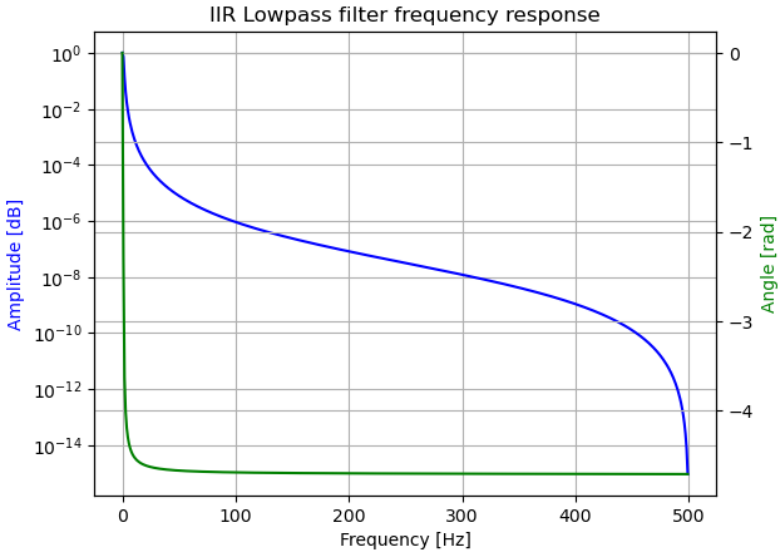

Figure 2.15: Frequency response of an infinite impulse response (Butterworth) low-pass filter. The filter has a f_{cut} of 1 Hz and has a length of 3. Notice how the phase delay is *not* linear and thus phase distortion is introduced

same as the standard deviation of the distribution [55]. In other words this means that RMS can extract the signal power of all frequencies in a signal in the time-domain if the frequencies are normally distributed. Since the probability density of surface EMG is approximately Gaussian, RMS should theoretically be the maximum likelihood estimator of EMG amplitude [50].

$$RMS = \sqrt{\frac{1}{n}(x[1]^2 + x[2]^2 + \cdots + x[n]^2)} \tag{2.16}$$

2.6 Standard sEMG signal processing

A conventional static real-time sEMG signal processing chain is described in [56]. The relevant steps are as follows:

- Remove DC component from signal
- Band-pass filter 20-300 Hz
- Notch filter at 50 Hz
- Half-wave rectification
- Low-pass filter for envelope detection

This signal processing chain will also be tested in this report and compared to alternative techniques.

2.7 Conclusion

In this theory section the required background information is given to understand the simulations, measurements, and conclusions that are discussed in this report. For each processing step, multiple processing methods have been discussed all of which can be seen in Figure 1.1, and information about the relevant parameters has been given. For the Wiener filter and the adaptive LMS filter a mathematical derivation is presented.

3 Simulation

This section of the report describes the testing of separate signal processing steps in a simulated environment. Each block as seen in Figure 1.1 will be tested individually, and the method and results will be discussion on a per-block basis:

- Pre-whitening
- Filtering
- Envelope estimation

Unless specified otherwise all signals will be high-passed with an f_{cut} of 1 Hz to remove DC bias before any operation is applied

3.1 Pre-whitening

A whitening filter is a digital filter with a frequency response that is (ideally) the inverse of the frequency contents of an sEMG signal.

3.1.1 Method

A testing signal was created that approximates the frequency response of an sEMG signal. The testing signal was created by creating a long white noise signal and multiplying the amplitudes in the frequency spectrum with a curve that estimates the frequency response of an sEMG signal. After this the signal is passed through inverse fft to go back to a time-domain signal. The result can be seen in 3.1 subplot 1 and 2.

The whitening filter is then created by taking the FFT of the time-domain test signal and taking its reciprocal at every frequency. Lastly the whitening filter frequencies are multiplied by the mean of the original signal frequencies to make sure that when the filter is applied the mean stays the same. These steps can be seen in 3.1 subplot 3.

3.1.2 Results

Figure 3.1 shows the whitening filter that functions as expected. In the center subplot the 'ideal' result are shown (multiplication in the frequency domain), and in subplot 5 the result from convolution in the time domain is shown. In subplot 5 a smoothed version of the filtered signal FFT is added to display that the signal power has a mean that approximates white noise. This filter was made using a Savitzky-Golay filter with a window length of 31 and a polynomial order of 3.

3.2 Filtering

First the metrics are introduced that will be used to compare filter performance. Subsequently, the construction process of each filter is presented. Lastly the different filtering methods are compared.

3.2.1 Comparison metrics

Each filter will be tested using two metrics: SNR (eq 2.1) and Bandwidth (definition of this will be given shortly). All filters are linear time invariant which means the superposition principle can be used to simplify SNR calculations [57]. The superposition principle simply states that filtering the sum of two signals is the same as filtering the signals individually and adding the results. An illustration of this can be seen in 3.2.

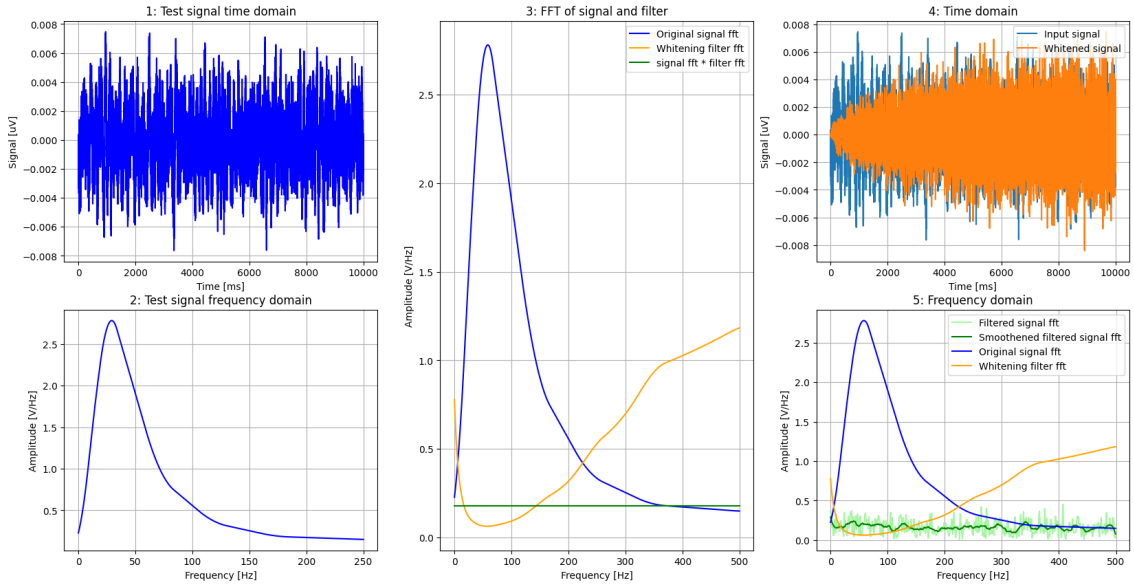

Figure 3.1: Subplot 1 and 2 display the input simulated input signal with a frequency response that approximates the frequency contents of an sEMG signal. Subplot 3 displays the frequency content of the signal, the subsequently calculated whitening filter, and the multiplication of the signal with the filter in frequency domain to show that the response is indeed white. Subplot 4 and 5 show the original and 'whitened' signal in time domain and frequency domain.

Due to the difficulty of creating a simulated signal that has the frequency contents of an sEMG signal and environmental noise, a pre-recorded sample of sEMG of a bicep going through maximum voluntary contraction was used to test the filters. This sample is not used for force estimation because it will not be compared to the contraction of an antagonistic muscle and purely the frequency contents of the signal are of interest. The sample that is used can be seen in Figure 2.2. Noise is taken to be 0 s to 2 s and signal is taken to be 5 s to 7 s. The RMS of the filtered signal is divided by the RMS of the filtered noise to create a signal to noise ratio.

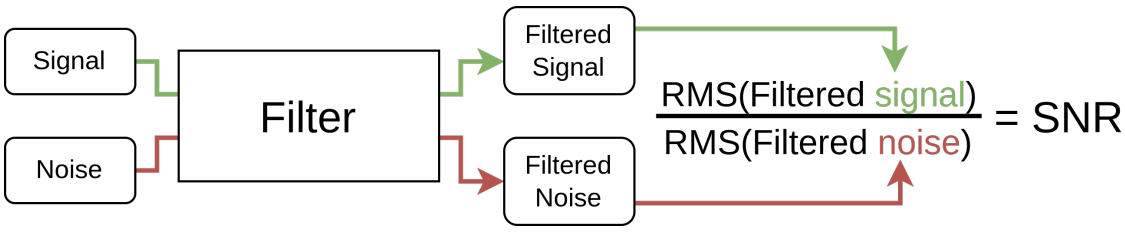

Figure 3.2: Illustration of testing of filters. Signal and noise are passed through the filter individually and the SNR is calculated for each filter.

SNR by itself is not a valid metric for judging a filters performance in this scenario. The purpose of improving SNR is the assumption that force can be estimated more accurately from a signal that contains primarily the signal generated by muscle contraction. However, a filter may be able to attenuate the signal and noise in such a way that the SNR is very high, but the signal is attenuated to such a degree that it no longer resembles the original signal that was generated by the muscle contraction. An example of this can be seen in Figure 3.3.

A measure to define how much the frequency spectrum has changed is the bandwidth. Typically the bandwidth of a signal is defined as the range of frequencies between two frequency points outside of which the signal is attenuated more than a specific threshold value [58]. This

definition is not applicable to this problem as the frequencies that are 'present' in an sEMG signal are not necessarily consecutive. Therefore the bandwidth of an sEMG signal will be defined as the number of frequency components that are larger than the mean of the frequency spectrum, a mathematical definition is given in Equation 3.1. With this metric, a frequency spectrum such as the one seen in Figure 3.3 will have a low bandwidth because most frequencies are below the mean.

$$\text{Bandwidth} = \#\{x \in \text{fft(sig)} \mid x > \overline{\text{fft(sig)}}\} \tag{3.1}$$

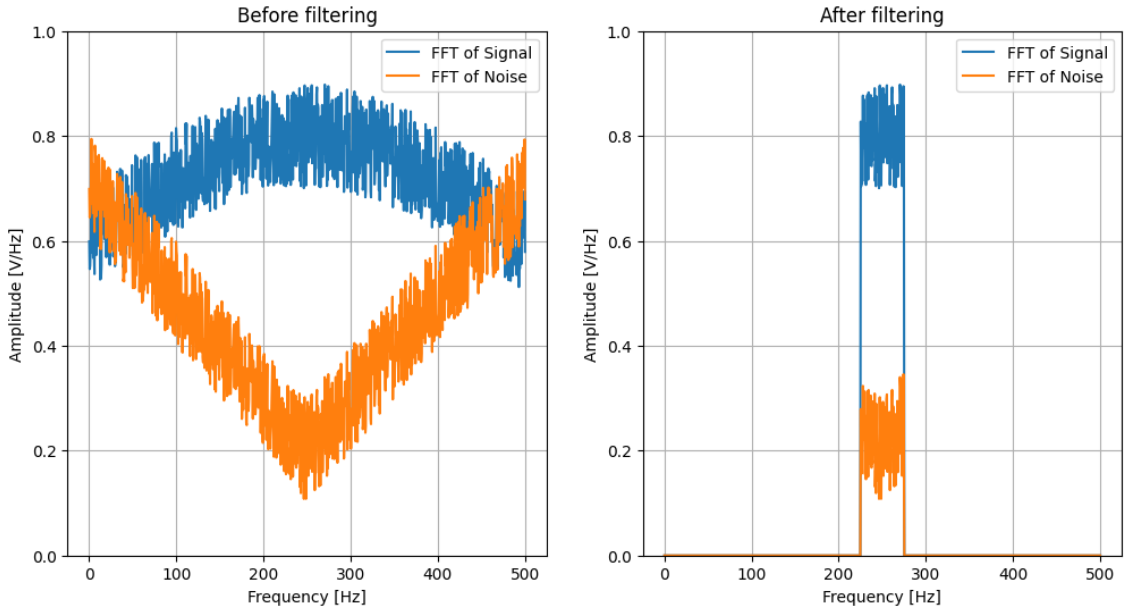

Figure 3.3: Example of filtering that results in good SNR but bad bandwidth.

3.2.2 Method

Static filter

The theory from section 2.6 specifies the removal of DC frequencies, a notch filter at 50 Hz, and a bandpass filter between 20 Hz and 300 Hz. Looking at the noise spectrum in Figure 2.3 it can be seen that there also exist significant peaks at 100 Hz and 150 Hz. Therefore different static filters were tested with different amounts of notch filters.

- IIR Notch filters at 50 Hz, 100 Hz, 150 Hz, 200 Hz. All have a Q-factor of 10, are constructed as numerator/denominator pairs and applied using scipy's lfilter.
- The bandpass filter consists of a high-pass filter with an f_{cut} of 20 Hz and a lowpass filter with an f_{cut} of 300 Hz. Both filters are of length 5, are constructed as numerator/denominator pairs, and applied using scipy's lfilter.

The frequency response of these filters can be seen in Figure 3.4. The resulting metrics can be seen in the chart 3.5.

Wiener filter

As discussed in section 2.3.1 the Wiener filter coefficients are constructed from the cross-correlation vector between signal+noise ($d(n)$) and the noise ($v(n)$) and the auto-correlation of the noise as is presented in the Wiener-Hopf equation in Equation 3.2 [32].

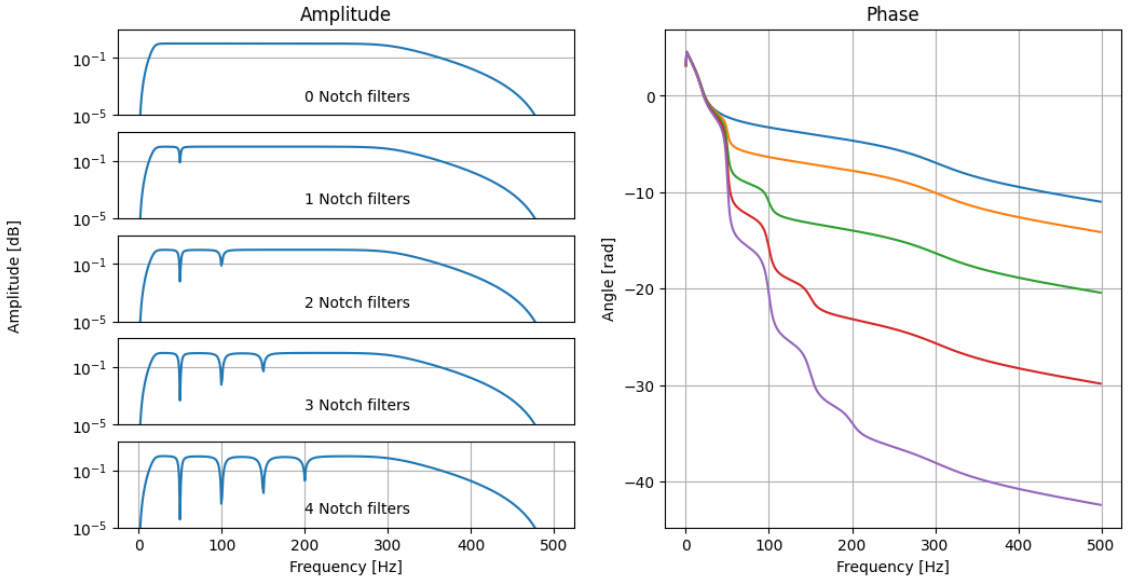

Figure 3.4: Frequency response of static filters with a different number of notch filters. The plots were created by determining the frequency responses of each individual filter (notches, low-pass, high-pass), then multiplying the amplitudes and adding the phase shifts. For the sake of illustration the amplitude graphs have been shifted vertically to clearly show the existence of notch filters in different lines, during simulations this shift was not present.

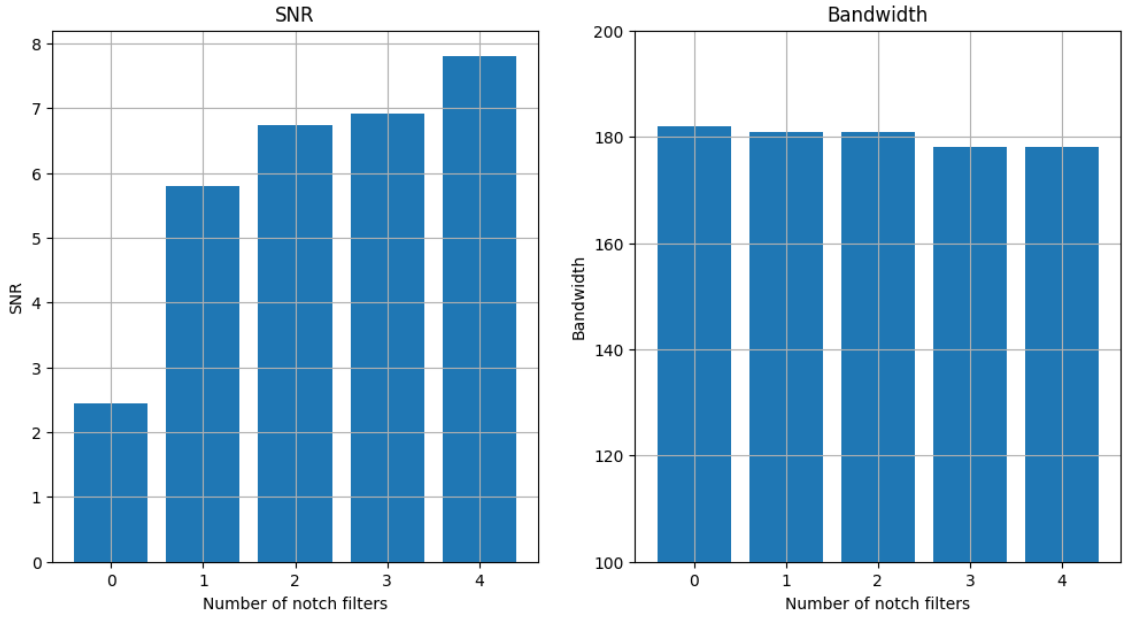

Figure 3.5: SNR and bandwidth of static filters with different numbers of Notch filters. Four notch filters were chosen for the measurement section (4) as the bandwidth seems to not depend very much on number of filters but the SNR seems positively correlated. Even though the peak around 200 Hz as seen in Figure 2.3 could is not as significant as other multiples of 50 Hz

it is still included because it *is* significant compared to the rest of the noise spectrum.

$$w_{\text{opt}} = R^{-1}P \tag{3.2}$$

The number of Wiener filter coefficients have a strong influence on the performance of the filter as can be seen in Figure 3.6. For the measurements section (4), a Wiener filter of length 500 was chosen as this is a middle ground for SNR and bandwidth.

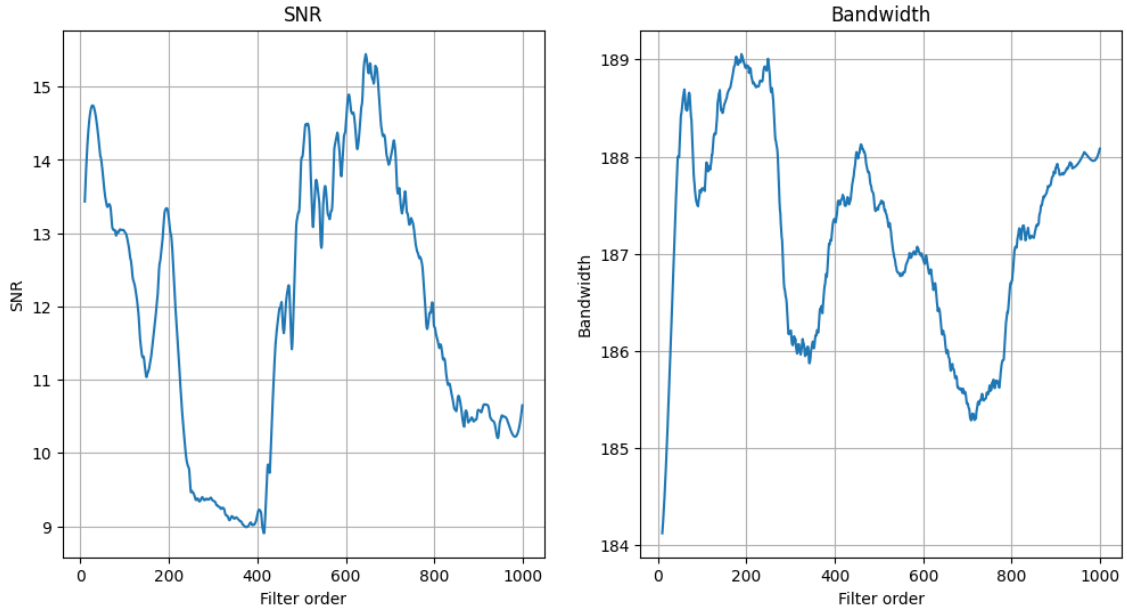

Figure 3.6: The effect of the number of Wiener filter coefficients on the SNR and bandwidth. To clarify the more general influence of filter length both plots were smoothed using a Savitzky-Golay filter with length of 71 and poly order of 3. It appears there is a clear peak in SNR at 650 filter terms but this corresponds to a low bandwidth. A filter length of 500 was chosen as this presents a good middle ground between SNR and bandwidth peak in the bandwidth.

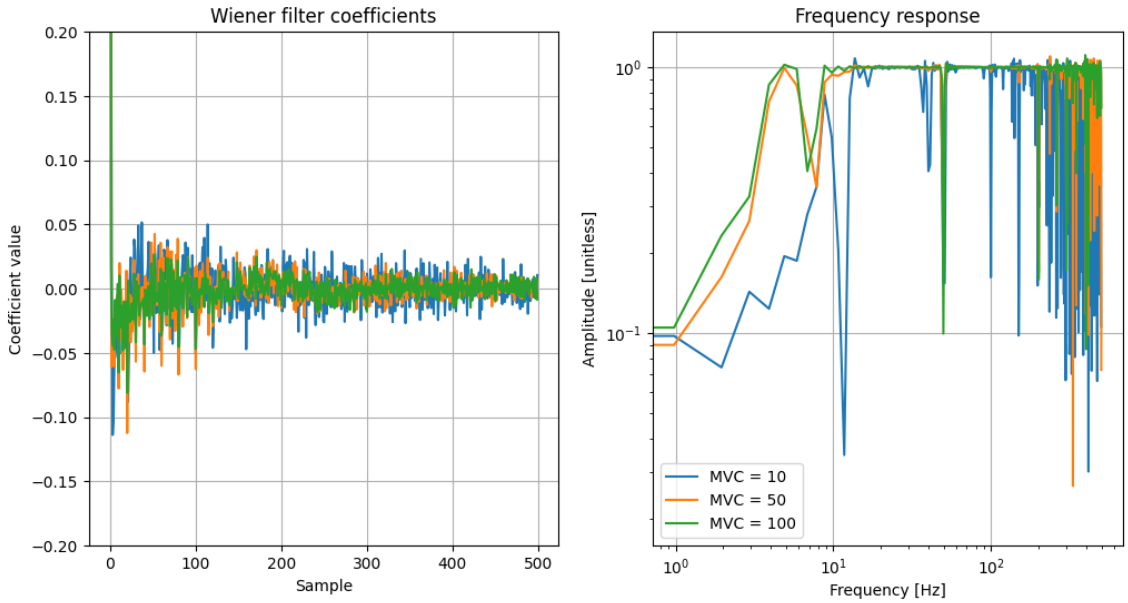

Figure 3.7: The frequency response of a Wiener filter at different levels of MVC. It can be seen that at a lower MVC the filter appears to have a very aggressive frequency response (seen by the large peaks at 10 Hz and higher frequencies) while at higher MVC this response is much less pronounced.

Adaptive filter

The functioning of an LMS filter has been described in the theory section 2.3.1. An LMS filter has two properties that determine its behaviour: The filter length and the convergence coefficient. To determine the best combination of these parameters when applied to sEMG signals a range of different values was tested. The results can be found in Figure 3.8. For the measurement section (4) an LMS filter with length 500 and convergence value of 0.1 will be used.

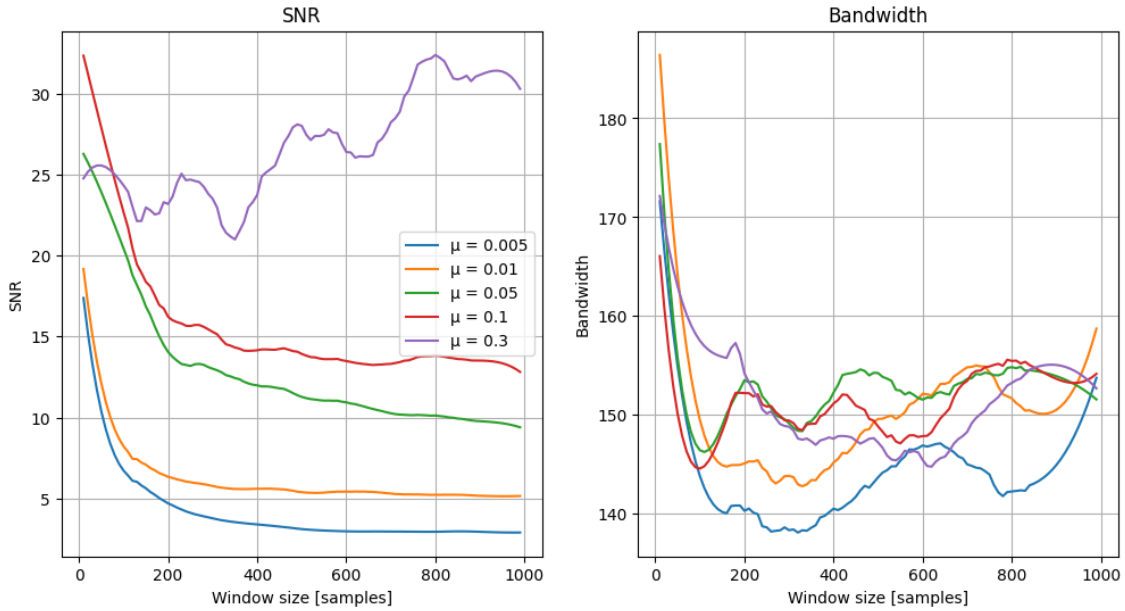

Figure 3.8: SNR and bandwidth of an adaptive LMS filter using different combinations of filter length and convergence value. It should be noted that each signal has been smoothed using a Savitzky-Golay filter with a window length of 31 and a polynomial order of 3. This is done to make the difference in performance between different convergence values clearer as without filtering the signals have a larger deviation that makes the lines unreadable. A higher convergence value seems to result in a better SNR. Furthermore it seems that increasing window length results to lower SNR (except for the convergence value of 0.3), but to slightly higher bandwidth. The convergence value of 0.1 stands out as it seems to increase with window size, but in practise this results in a larger error due to the swinging behaviour that was discussed in the theory section 2.3.1. A convergence value of 0.1 with a filter length of 500 was chosen as this yields a good middle ground between SNR and bandwidth

3.2.3 Results

A property that might be of interest is each filters performance in different levels of Maximum Voluntary Contraction (MVC). This allows for insight into how well each filter functions in different levels of signal compared to the environment noise. This was realized by keeping the noise constant, but scaling the signal to different levels (from 1-100 %) to simulate different levels of MVC. The SNR of the filtered signal and filtered noise was divided by the reference SNR (SNR of input signal and input noise) to be able to draw a clear conclusion about the filters performance. This has as effect that the unfiltered signal results in a horizontal line with the value of 1 as can be seen in 3.9.

Again, the bandwidth was calculated for different filters and at different levels of MVC. The results can be seen in Figure 3.10.

For bandwidth holds that the metric is independent of degree of muscle contraction as seen in Figures 3.10 and for SNR this holds except for the non-static adaptive LMS filter as seen in

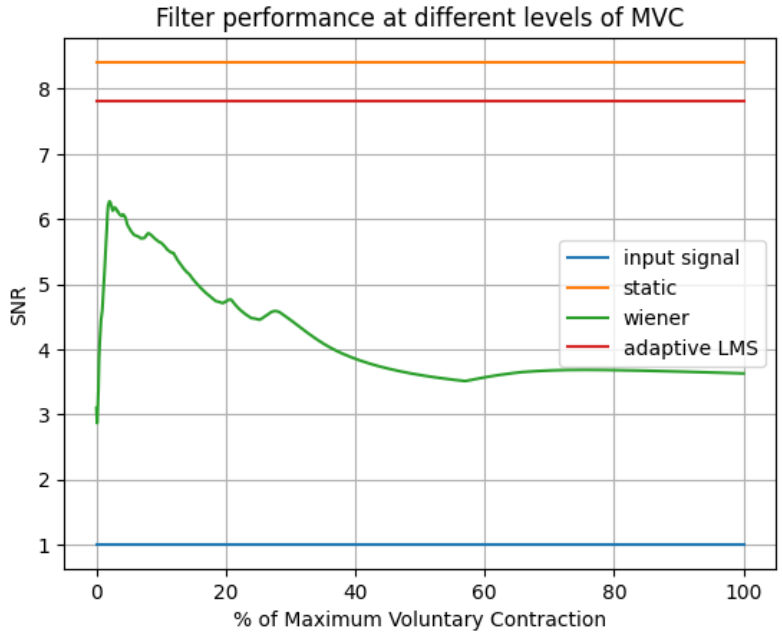

Figure 3.9: The normalized SNR of each filter for different levels of MVC (filter SNR divided by unfiltered signal SNR). It can be seen that there is no relation between the static and adaptive filters performance and the degree of contraction. An interesting observation can be made about the Wiener filter as it seems to perform better at lower MVC. This could be explained by the fact that if noise makes up a larger portion of the signal it might be 'easier' to find a set of filter coefficients that filter a larger portion of noise away. If a few frequencies in the noise are orders of magnitudes larger than those frequencies in the signal, a filter that removes that frequency will impact the noise much more than the signal which results in a higher SNR. It can also be seen that the SNR of the Wiener filter is much lower than the numbers presented in Figure 3.6, this may be caused because the plots shown in Figure 3.6 have been smoothed to reflect general behaviour. Without this smoothing, the plot in Figure 3.6 has a large deviation and it is possible that this specific filter length was not great for this specific signal but, given a larger data set, will approximately follow the results presented in Figure 3.6.

Figure 3.9 Figure 3.9 shows that the best signal to noise ratio is achieved using a Wiener filter, but this filter also has the worst bandwidth performance as seen in Figure 3.10.

3.3 Envelope estimation

3.3.1 Comparison metrics

There are two separate metrics that need to be measured when comparing envelope estimation techniques. The first one is how 'fast' a techniques is, and the second is how 'good' the technique is. The first metric gives information about how much the 'detected' signal lags behind the 'true' signal. The second metric is the quality of the envelope estimate when accounting for the lag.

The lag is detected by calculating the cross-correlation between the true signal and the envelope estimate. Cross-correlation is a metric that determines the similarity between two signals as a function of displacement of one signal relative to another [59]. Since the 'true' signal and the estimated signal are most similar when their displacement equals the lag, a detectable peak is formed in the cross correlation function. The left subplot in Figure 3.11 displays a 'true' signal (measured force), and a simulated estimation of this signal (estimated force) that lags behind the true signal. The cross-correlation is also plotted that has a peak at 100 ms, which is the exact amount of lag between the two signals. The right subplot shows the two signals where the estimated signal has shifted to account for the lag.

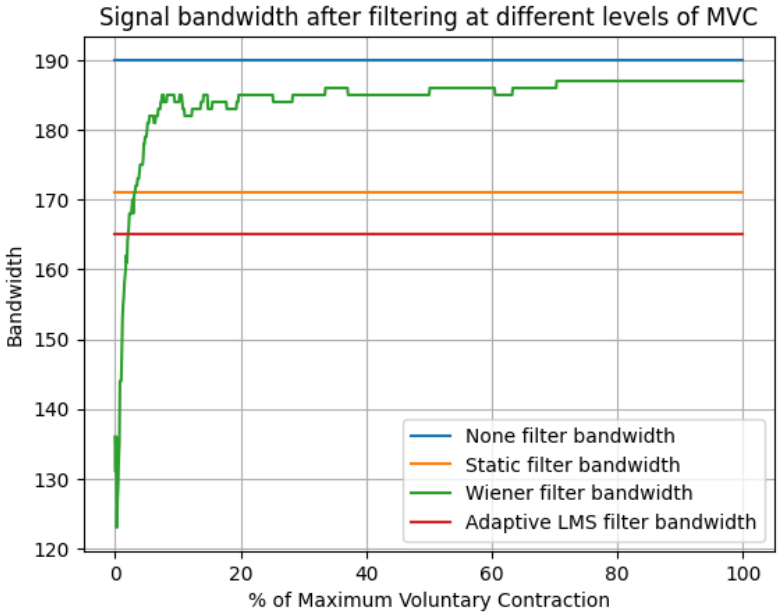

Figure 3.10: The bandwidth of each filter for different levels of MVC. It can be seen that there is no relation between a filters performance and the degree of contraction for the static and adaptive filter. The static filter performs as expected as it removes the same frequency components regardless of the amplitude of the signal. The Wiener filter seems to have larger bandwidth at higher MVC. This can logically be explained by the fact that the optimal filter uses the statistical spectral properties of the entire signal sample, but in situations of low MVC may not result in good filtering on subsets of the signal. The adaptive filter does not have this problem as it can adjust the filter terms to also accurately filter subsets of the data.

The error can be determined by subtracting the true signal from the estimated signal, and the root-mean-square-error can be calculated.

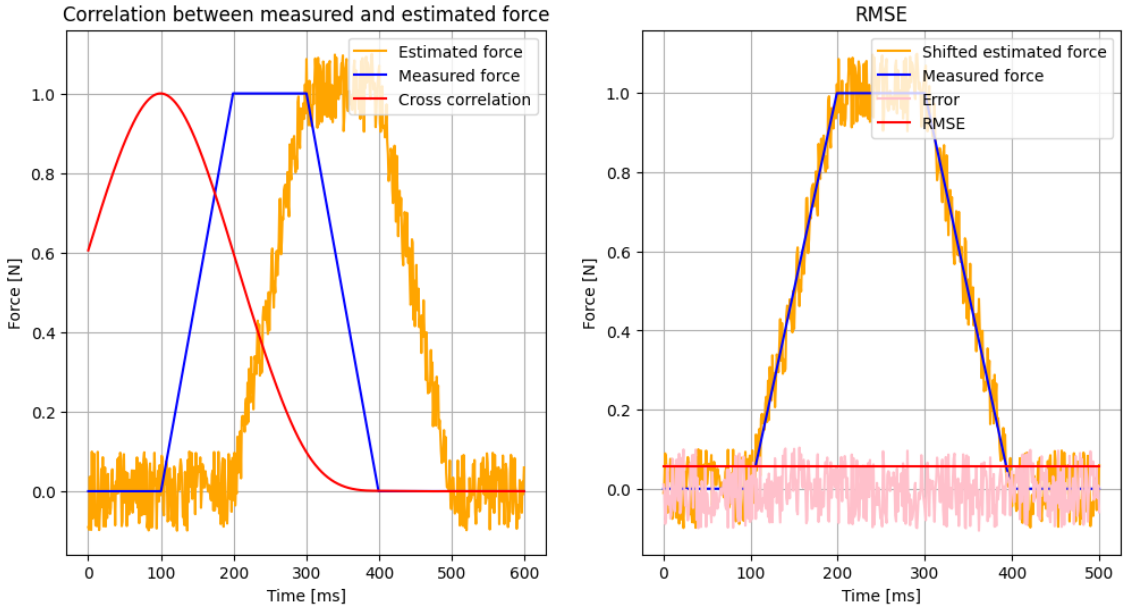

Figure 3.11: Illustration of method for judging envelope estimation

An input signal was generated to be Gaussian white noise since it has signal properties close to that of an sEMG signal, and is multiplied with a modulation that can be seen in the left subplot of Figure 3.12. The envelope detection techniques are applied onto the input signal and the results are plotted in the right subplot of Figure 3.12.

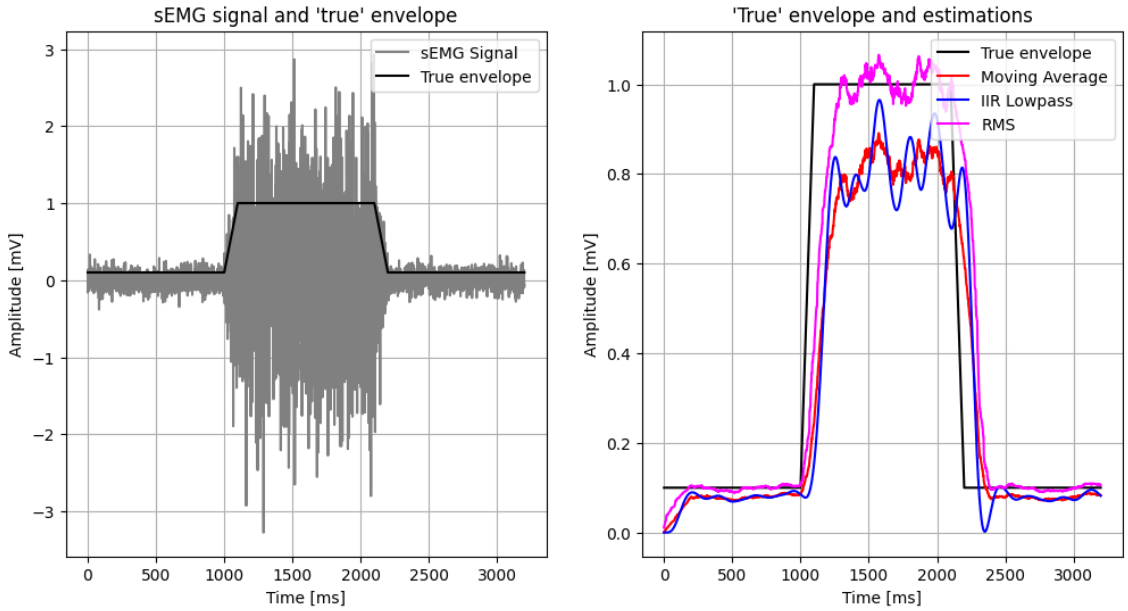

Figure 3.12: Left: Input signal and 'true' envelope'. Right: Envelope detection using different techniques to illustrate difference in behaviour

3.3.2 Method

IIR lowpass filter

A Butterworth filter was used to construct an IIR lowpass filter. The performance of such a lowpass filter is defined by its f_{cut} and the number of filter coefficients (or the filter order). The highest frequency that the envelope should be able to produce is the frequency by which one can contract and relax the measured muscle. It was empirically determined that the maximum frequency for switching between total relaxation and maximum voluntary contraction and back was around 5 Hz and thus the f_{cut} was varied from 1 Hz-9 Hz. The filter length was varied from 2-8 because the minimum possible filter length is 2 (a single filter coefficient provides no filtering, just scaling the signal with a constant), and a filter length >8 resulted in unstable behaviour. A plot of the frequency response of the IIR Butterworth filter can be seen in Figure 3.13. The filters are achieved as a numerator/denominator sequence. Since the purpose of this filter is real-time envelope detection, it was applied using scipy's lfilter since as that is causal forward-in-time filtering only.

Moving average

The moving average filter only depends on the length of the filter, Figure 3.14 depicts the frequency behaviour of the moving average filter of different lengths. The range of values that are tested is chosen arbitrarily, but large enough to cover general use cases.

Root mean square

Similar to the moving average filter, the behaviour of the RMS filter is solely determined by the length of the filter. The same range of filter lengths was chosen as for the moving average filter so that the performance could be directly plotted against each other.

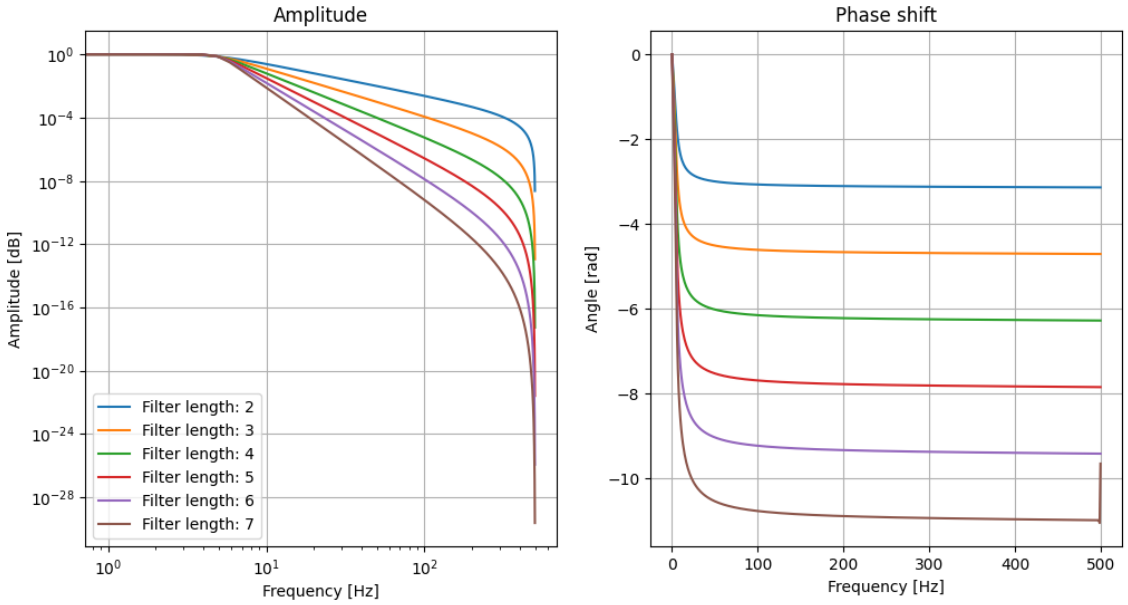

Figure 3.13: Frequency response of IIR Butterworth filter of different order. The f_{cut} was set to 5Hz.

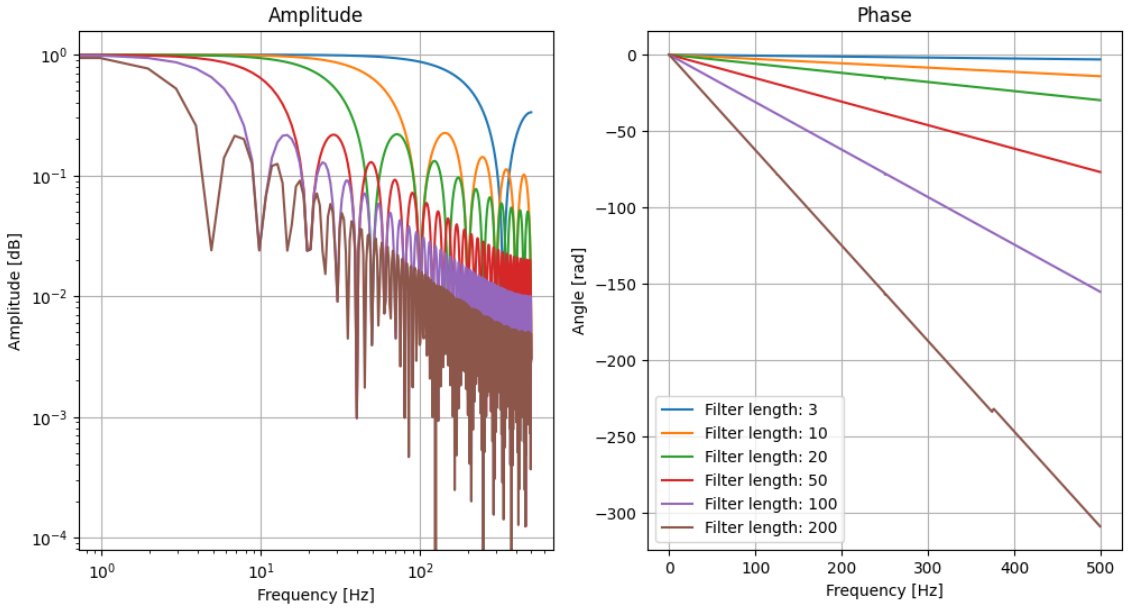

Figure 3.14: Frequency response of moving average filter of different lengths. The coefficients of the moving average filters are 1/length of filter.

3.3.3 Results

To properly evaluate the performance of the envelope detection techniques each method has been tested individually across the range of variables that were described in the previous method section and plotted against the resulting lag and error.

The graph describing the performance of the IIR Butterworth filter can be seen in Figure 3.15. The graph describing the performance of the moving average filter and the RMS filter can be seen in Figure 3.16.

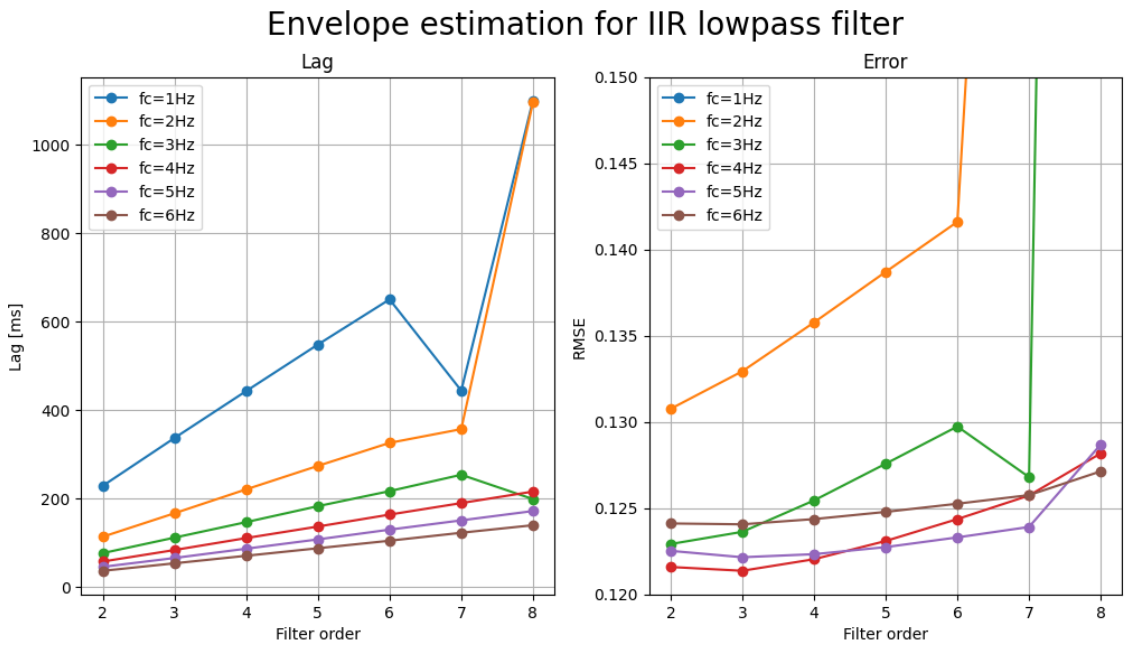

Figure 3.15: Lag and error of an IIR Butterworth filter for different cut-off frequencies and filter lengths. Note that filters with a lower f_{cut} and high number of filter coefficients become unstable which can be seen in the error-graph for cut-off frequencies 1 Hz-3 Hz. Additionally, the error in these graphs are all below 0.125. This is caused by the fact that the modulation is between 0 and 1, the error is <1 and the squared error is smaller still. So not the error value, but the *relation between* error values of different methods is the truly useful information here.

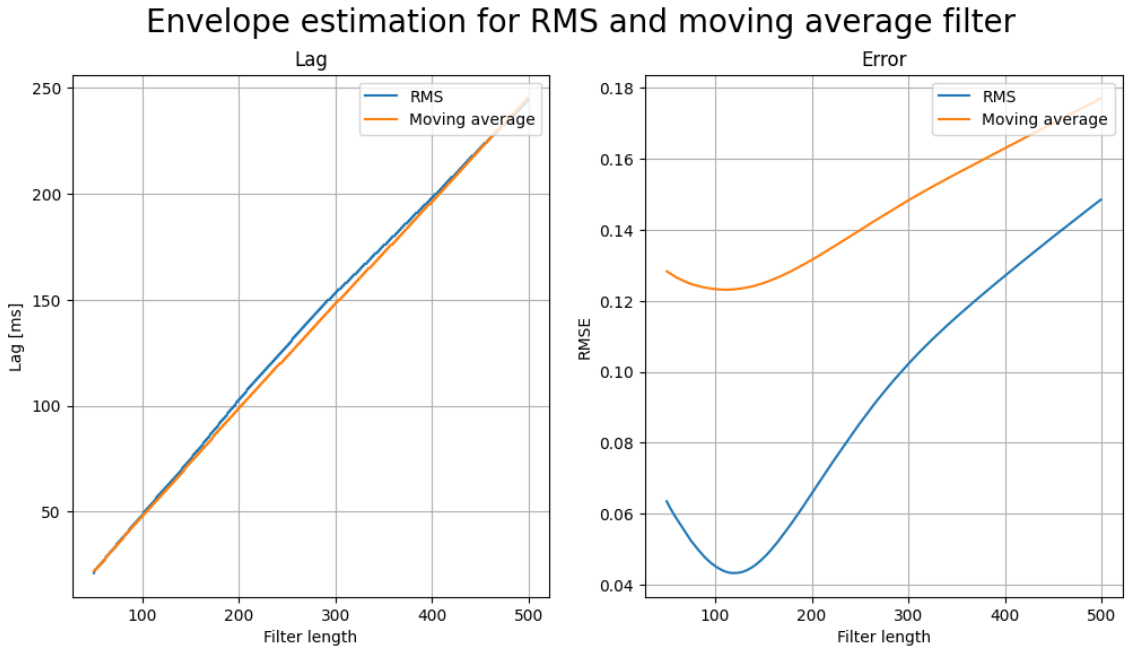

Figure 3.16: Lag and error of RMS filter and moving average filter for different filter lengths

From Figure 3.15 it can be seen that an IIR LP Butterworth filter of length 3 and f_{cut} of 4 Hz results in the lowest error. A filter with f_{cut} of 6 Hz has the lowest lag but this is only marginally

less than a f_{cut} of 4 Hz. For this reason an IIR LP Butterworth filter of length 3 and f_{cut} of 4 Hz is used in the the measurement section (4).

From Figure 3.16 it can be seen that moving average and RMS methods have similar lag, and the lag has a linear relation to the filter length. In the same figure it can also be seen that the error reaches a minimum at a filter length of 120. For this reason both the RMS and moving average method are applied with a filter length of 120. The Figure also shows that the error increases with more filter terms which may seem counter-intuitive. A possible explanation for this is that filters with more filter coefficients can achieve a higher transition bandwidth. As a result, the envelope may be detected through a sets of frequencies that does not accurately represent the applied force. Shorter filters have smaller transition bandwidth and thus a 'smoother' frequency range is used to construct the envelope.

3.4 Force estimation

The measured sEMG signals from antagonistic muscles needs to be combined to form an estimate of the exerted force. Since this calculation is done in a consistent way throughout all measurements this section serves purely to provide some insight into the method of calculation.

The previous step of envelope estimation is used to get a measure of muscle activation. Since muscle activation leads to muscle contraction and exerted force around a joint is the difference between how much antagonistic contract [4] it becomes possible to determine the force from sEMG. To correlate the difference in muscle contraction from antagonistic muscles (such as biceps and triceps) to the exerted force, the muscle contraction needs to be scaled. As previously mentioned, a linear relation between sEMG and force will be assumed [7] [6]. In Figure 3.17 it is shown how the exerted force is estimated from simulated bicep and triceps sEMG.

3.5 Conclusion

In this chapter different filtering and envelope detection methods were compared. For each method, different variations of parameters were tested to determine the most optimal solution for each option. From the presented simulations the following expectations are made:

- The static filter performs the best in terms of SNR, but in terms of bandwidth performs worse than other filters. The unfiltered signal yields the largest bandwidth but the lowest SNR. From this it is expected that if a high SNR results in a more accurate force estimation from sEMG that the static filter will perform best in force estimation as long as the MVC is large as seen in Figure 3.9, but if MVC is small then the adaptive LMS filter is expected to perform best.If bandwidth is the most important property for estimating force from sEMG it is expected that unfiltered signals perform the best, closely followed by the adaptive LMS filter and Wiener filter.

- The RMS envelope detection method results in the smallest error compared to moving average and IIR Low-pass filter for the determined filter parameters. In terms of lag the RMS envelope detection performs about the same as the moving average envelope detection, and both of these are expected to result in less lag than IIR LP filter.

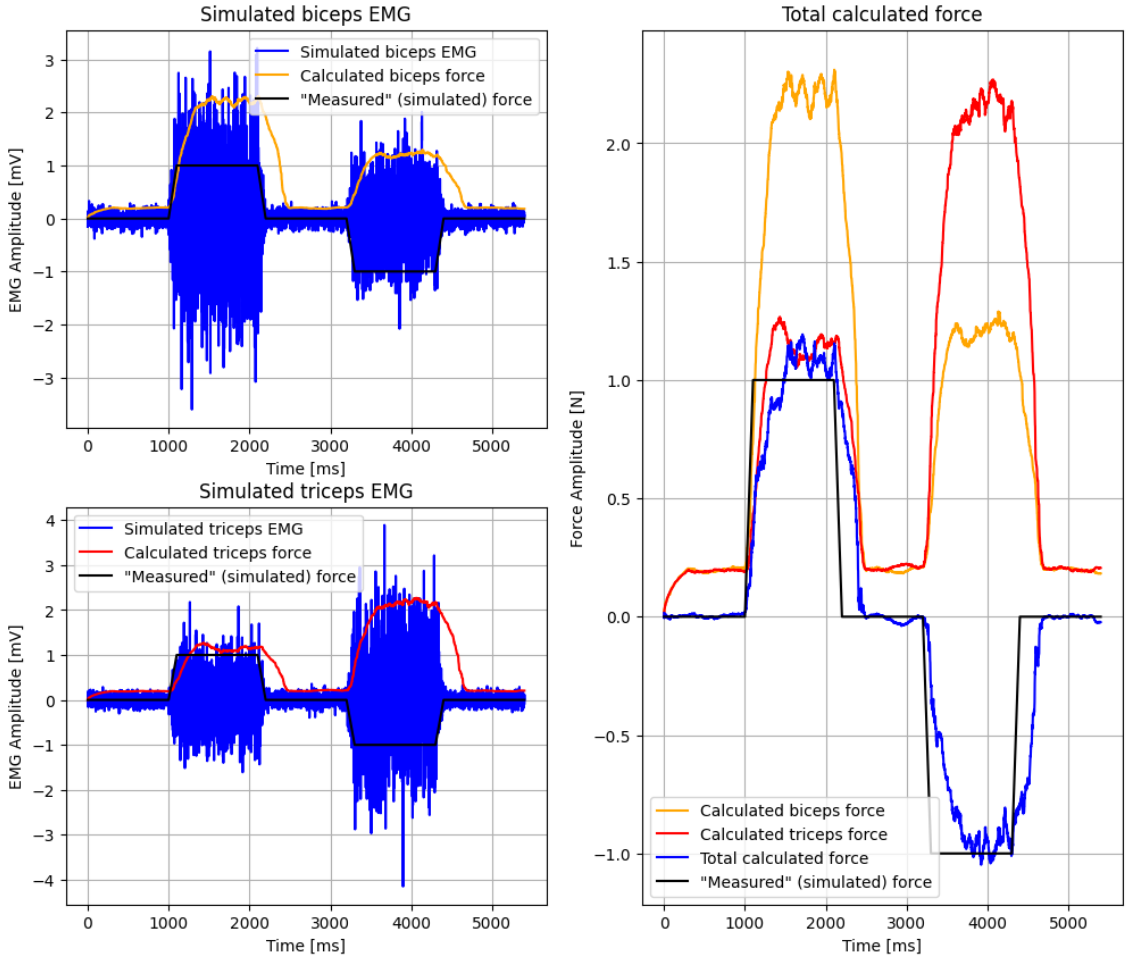

Figure 3.17: Process of estimating force from simulated sEMG (random Gaussian noise). The bicep envelope is calculated at the top, notice how during downwards force exertion the bicep still activates but to a lesser degree than during upwards force exertion. The same holds for the triceps in the bottom figure. The subplot on the right shows the envelope of the bicep, triceps, the difference between these two (identical to estimated force assuming linear scaling with factor 1), and the 'measured' force .

4 Measurements

This chapter aims to validate the accuracy of force estimation from sEMG after different processing techniques by comparing it to measured data. The goal is to measure sEMG from biceps and triceps, record the sEMG reference noise and to measure the estimated force using a load cell during an exercise of isometric contraction. The sEMG data is then processed using the different techniques that are discussed in the simulation chapter, and the final estimated force will be compared to the measured force.

4.1 Experimental setup

The measurement setup consists of the following components:

- Siemens Single Point Load Cell, 20 kg Range, Compression Measure
- Keysight E3631A DC power supply at 2 V to power the load cell
- TMSi Refa8-16e 16 channel amplifier
- Kendall H124SG Foam-Hydrogel ECG Electrodes

The 16 channel amplifier performs uni-polar measurements. This means that each electrode is connected to its own amplifier channel, and the measured values are compared to the value of a reference. The opposite of uni-polar is bipolar which entails that the potential difference between two electrodes is amplified by a single amplifier channel [60].

The load cell has 4 relevant terminals. Two terminals are connected to the power supply to supply the load cell with power. The other two terminals are connected to the amplifier. The 'common' terminal of the power supply is connected to the 'Patient ground' on the amplifier.

Sets of two electrodes are placed on the subjects right bicep, right triceps, and left arm. The electrodes were placed following SENIAM guidelines [61]. Two electrodes per set are chosen to be able to do a differential measurement. Since each electrode in a set measures almost identical sEMG signal the signals from the electrodes can be averaged to reduce any present noise. The electrodes on the left arm are used to record a reference noise. It is expected that this reference noise has an identical frequency spectrum as the noise present in the sEMG signal since it is recorded at the same time, approximately same place, using the same amplifier, and can therefore be used in some of the presented filtering techniques. The reference signal is recorded using a TMSi provided armband that was soaked with water (for better connectivity) and connected to 'Patient ground' on the amplifier. A total measurement setup diagram is shown in Figure 4.1. A photo of the measurement can be seen in Figure 4.2

A single long measurement was taken at a sampling rate of 1000 Hz where force was applied following a predetermined pattern. This measurement is accompanied by a calibration measurements where an object with known weight was attached to the load cell at the sampling frequencies.

The applied force followed the following pattern:

- Slowly pulling the handle upwards followed by a slow pushing the handle downwards. Repeated three times
- Slowly pull the load-cell upwards followed by returning to a neutral position. Repeated three times
- Slowly push the load-cell downwards followed by returning to a neutral position. Repeated three times

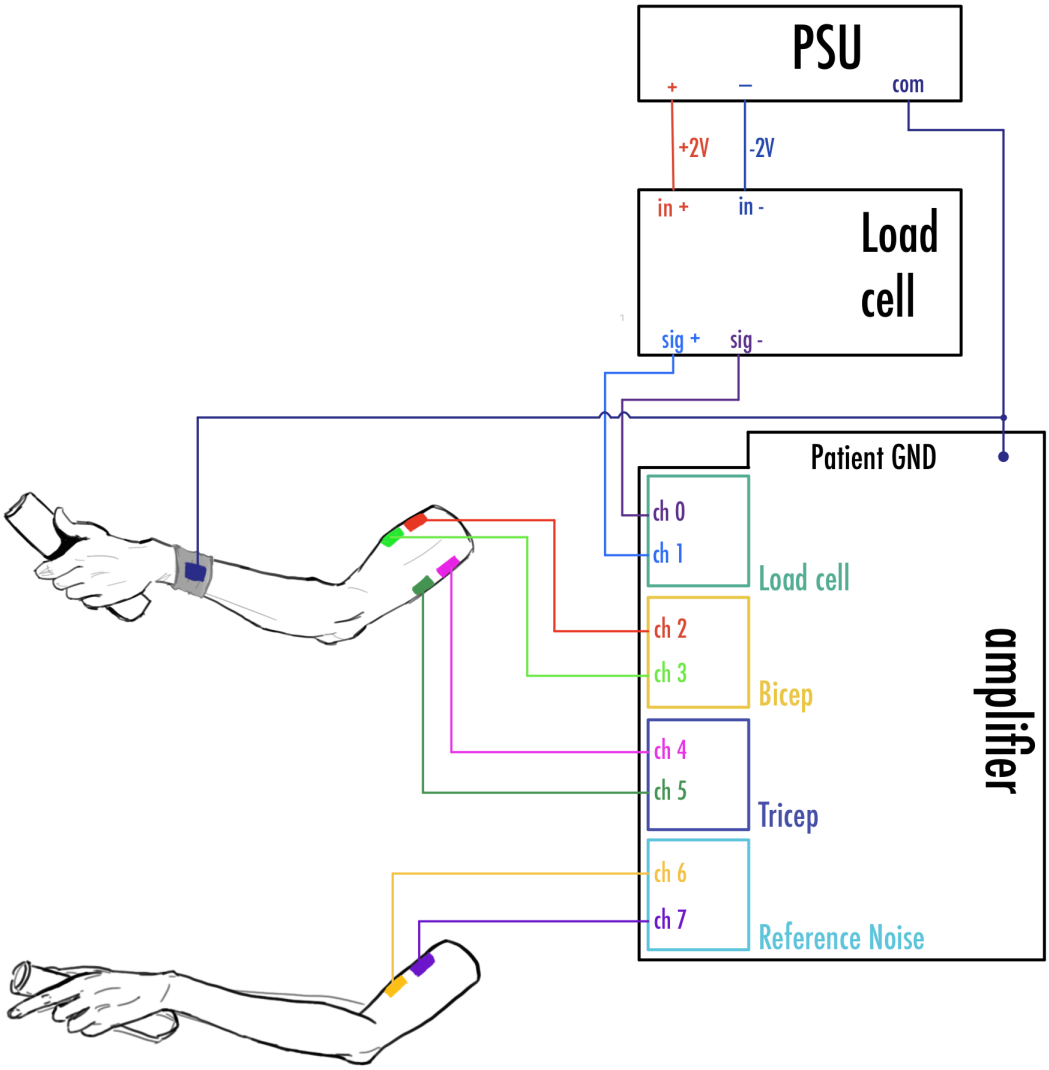

Figure 4.1: Diagram of the measurement setup

- Quickly pull the handle upwards followed by a quick push of the handle downwards. Repeated three times

4.2 Measurement data

The following configuration parameters were chosen based on simulation results:

- Whitening: A whitening filter was created from the signal spectrum between 5 and 10 seconds in Figure 4.4. The number of coefficients was limited to 500.
- Filtering
  - Static filter: 3 notch filters at 50 Hz, 100 Hz, and 150 Hz with q-factor of 10, low-pass Butterworth filter with f_{cut} of 20 Hz and length 5, high-pass Butterworth filter with f_{cut} of 300 Hz and length 5
  - Wiener filter: 200 filter terms, filter was created from the bicep signal
  - Adaptive LMS filter: The filter length was 500 and the convergence value was 0.05
- Envelope detection

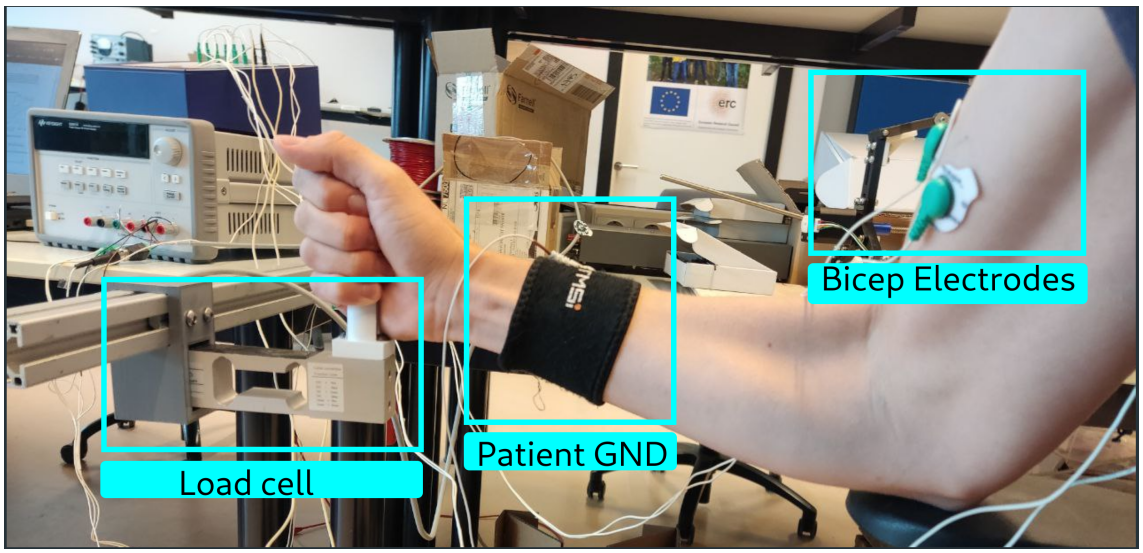

Figure 4.2: Picture of the measurement setup

- Moving average envelope detection: Length of filter was 120 terms
- IIR LP filter: f_{cut} of 4 Hz and a filter order of 3
- RMS: Length of filter was 120 terms

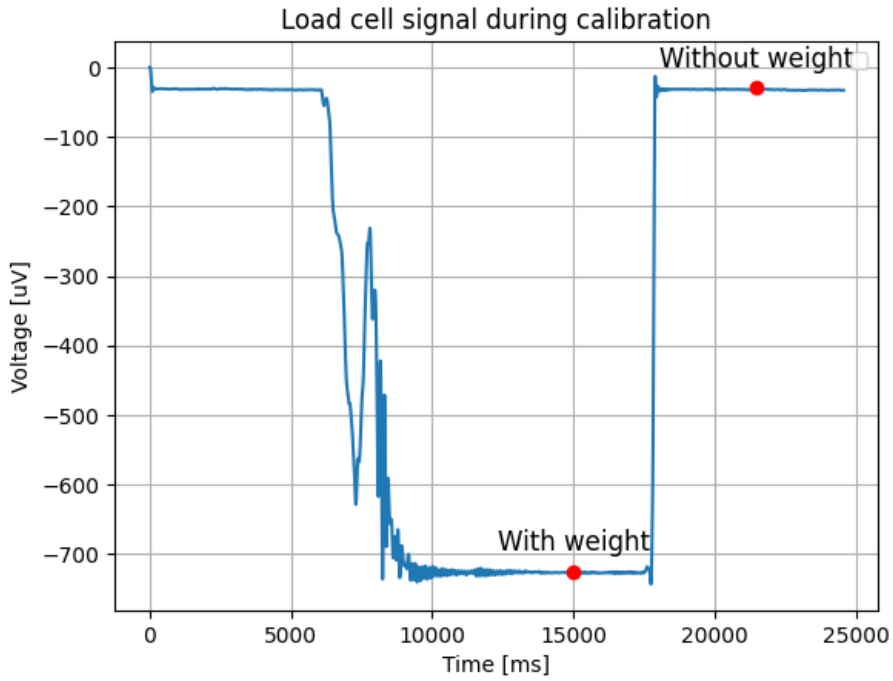

Figure 4.3: Calibration measurement at 1 kHz sampling rate. The force has been low-passed with an f_{cut} of 10 Hz to remove large 50 Hz noise component. The offset was determined to be −30 µV. The weight op the object was 1681 g which corresponds to a measured signal of 725 µV

.

The calibration was performed to determine what the relation between the measured voltage and the force was. A weight of 1681 g was attached to the measurement handle attached to the load cell which resulted in the measurement that can be seen in Figure 4.3. Through visual

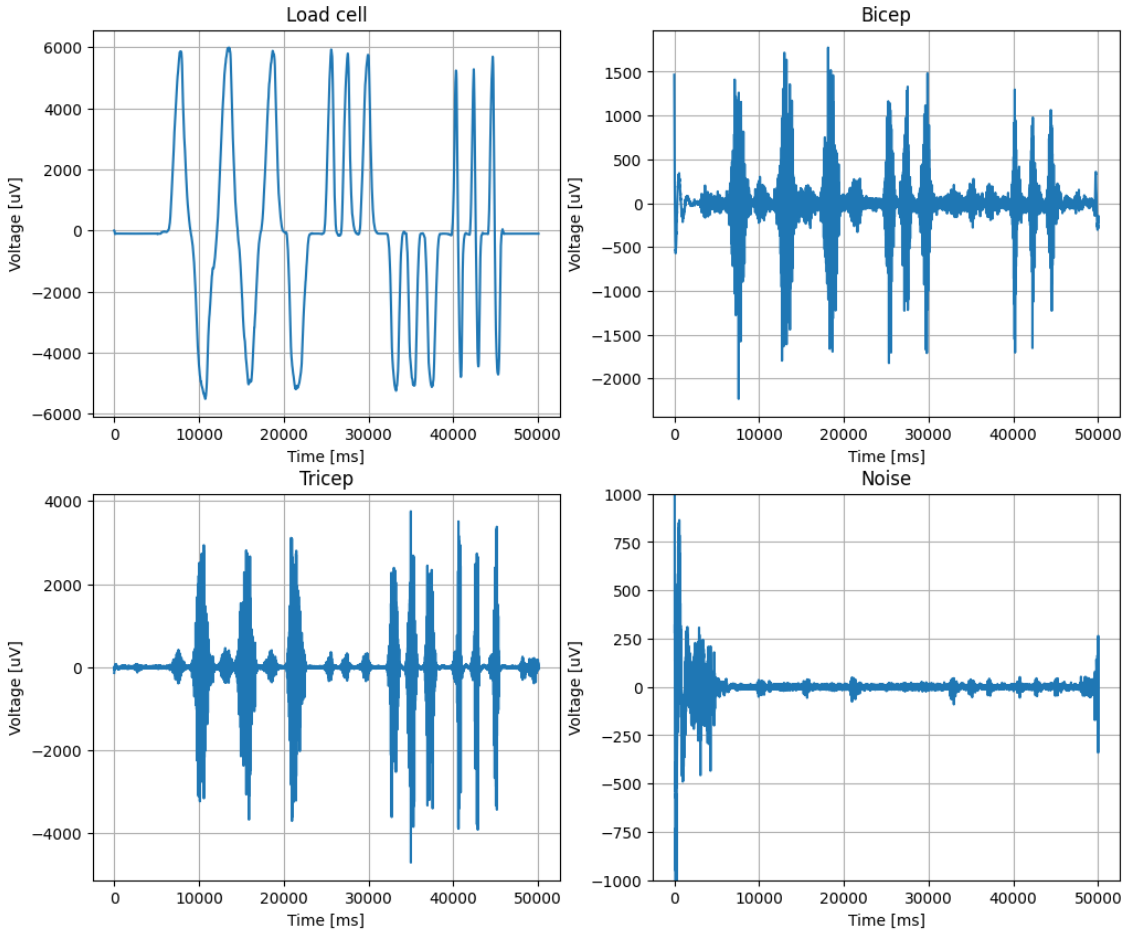

Figure 4.4: Force measurements and accompanying sEMG signals at 1 kHz sampling rate

inspection, the steady state offset of the setup without attached weight was determined to be 30 µV. After attaching the weight, the steady state voltage was determined to be 725 µV.

$$\frac{\Delta \text{weight [g]}}{\Delta \text{signal [mV]}} = \frac{1681}{7.25 - 0.30} = 0.00241[N/uV] \tag{4.1}$$

The measured force in Newton is approximately 0.00241 times the measured signal in micro Volt.

All measurements were performed in bipolar electrode configuration and the measurement for a set of two electrodes was found by adding the results together. This removes the average signal that is present in all signals.

4.3 Measurement processing result

All combinations of whitening, filtering, and envelope detection were applied onto the signals as seen in Figure 4.5. During processing it was noticed that some methods scaled the estimated force by large amounts and this resulted in high error rates. To still compare the accuracy of force estimation regardless of scaling factor the decision was made to intrude an intermediate step between measuring/compensating the lag and calculating the error. After accounting for the lag, a scaling factor is determined that minimizes the RMSE. The scaling factor is determined through the following algorithm:

- Calculate the RMSE

- Calculate the RMSE of a slightly amplified signal
- Calculate the RMSE of a slightly reduced signal
- Compare if amplifying or reducing the signal decreases the RMSE. If amplifying/reducing yields a lower RMSE, amplify/reduce the signal and repeat these steps. If amplifying and reducing both yield an RMSE lower than the current RMSE, the ideal scaling value has been found.

The estimated force is subsequently scaled by this scaling factor preparatory to calculating the RMSE value. For the RMSE calculation, the first 3 seconds and the last 3 seconds of the signals were discarded (after processing) because some processing steps did not yield their steady-state response in that time [62]. The results for lag, error, and scaling can be found in the bar-chart in Figure 4.5.

In Figure 4.5 it can be seen that whitening introduces significant lag. In the appendix are the results of constructing the whitening filter using zero-phase, linear-phase, and negative input signal phase A.3, A.2, A.1, A.4. If this were caused by the fact that the whitening filter was constructed using the phase of the input signal then it would be expected that using negative source phase this introduced delay would be counteracted, but as can be seen in appendix Figure A.2 this does not appear to be the case.

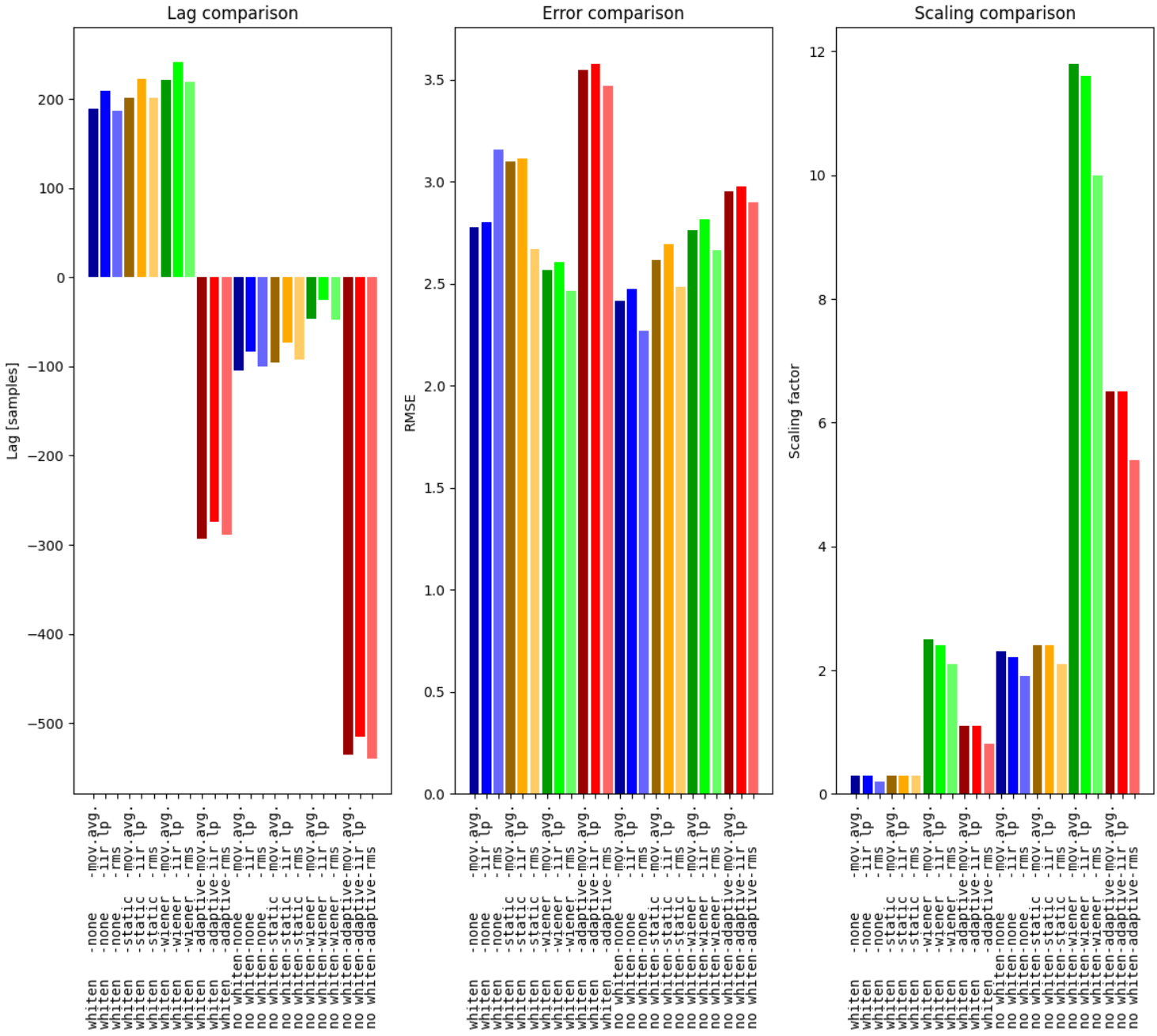

Figure 4.5: This plot contains all relevant results for all different combinations of whitening, filters and envelope detection

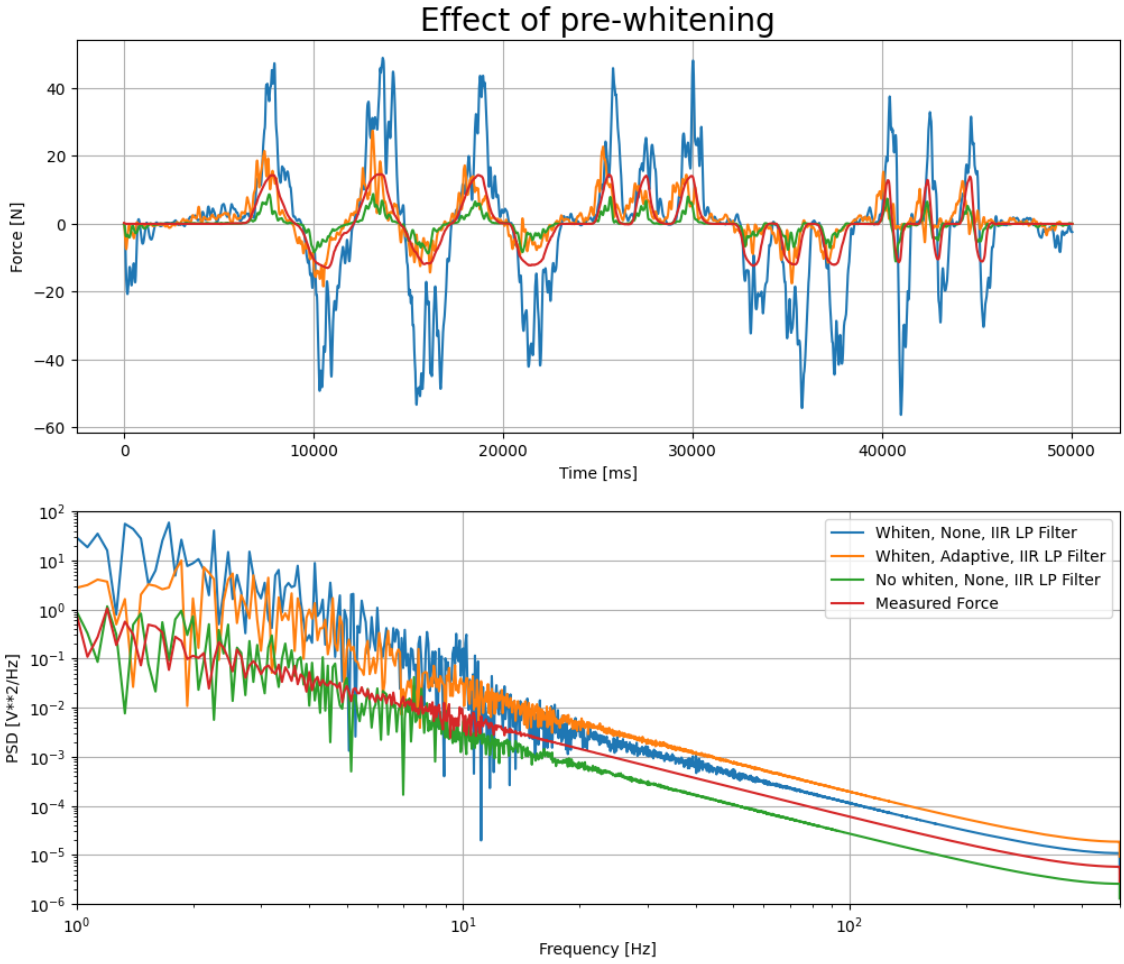

Figure 4.6: This figure illustrates the effect that whitening of the sEMG signal has on the resulting envelope. The signals were not filtered and moving average was used for envelope detection. Both unfiltered and adaptive filtered versions show volatile behaviour compared to the non-whitened variant. In the frequency domain it can be seen that whitening results in a spectrum of larger amplitude compared to the non-whitened spectrum which seems to follow the measured force much more closely

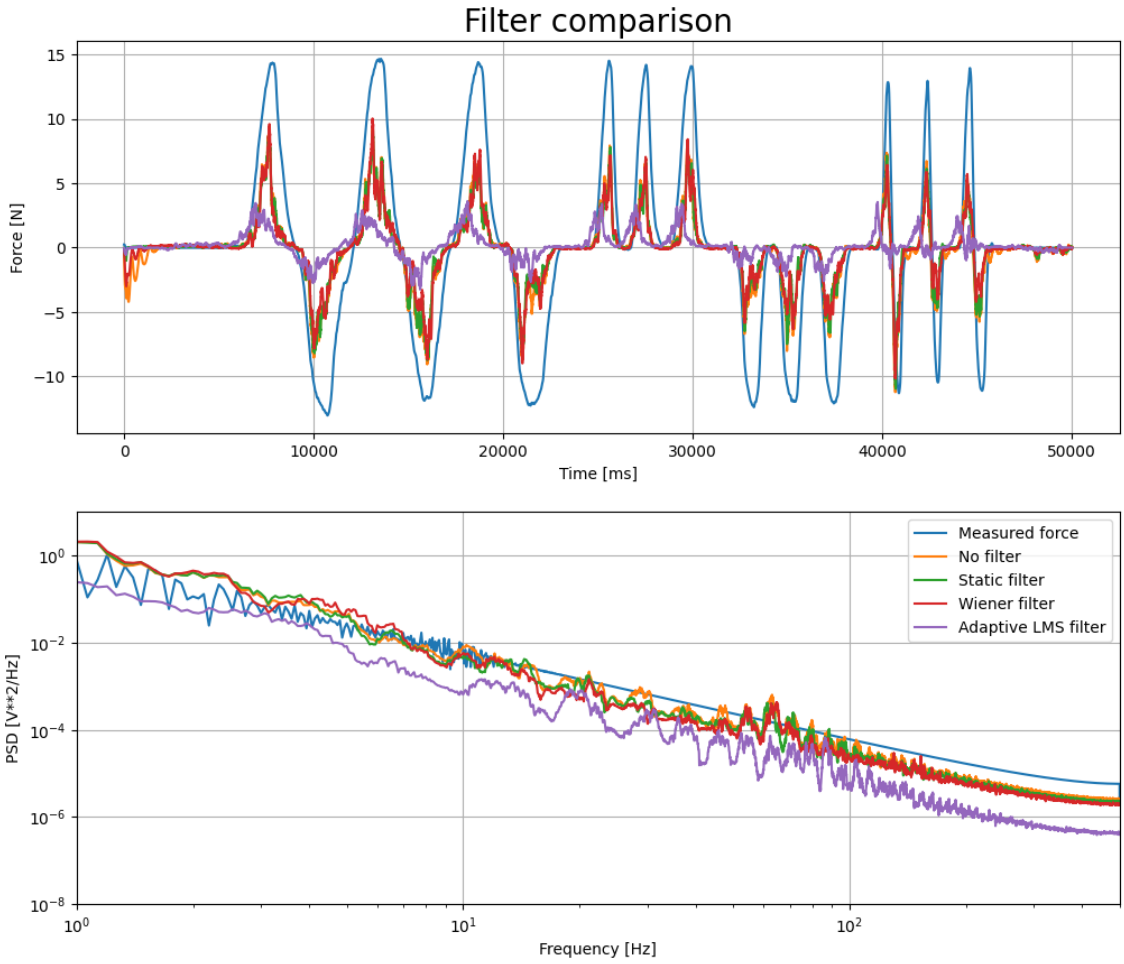

Figure 4.7: This figure illustrates the effect that different filtering techniques have on the resulting envelope. The signals were not whitened and moving average was used for envelope detection. The frequency plots have been smoothed using a moving average filter of length 10 to clearer show the difference in behaviour.

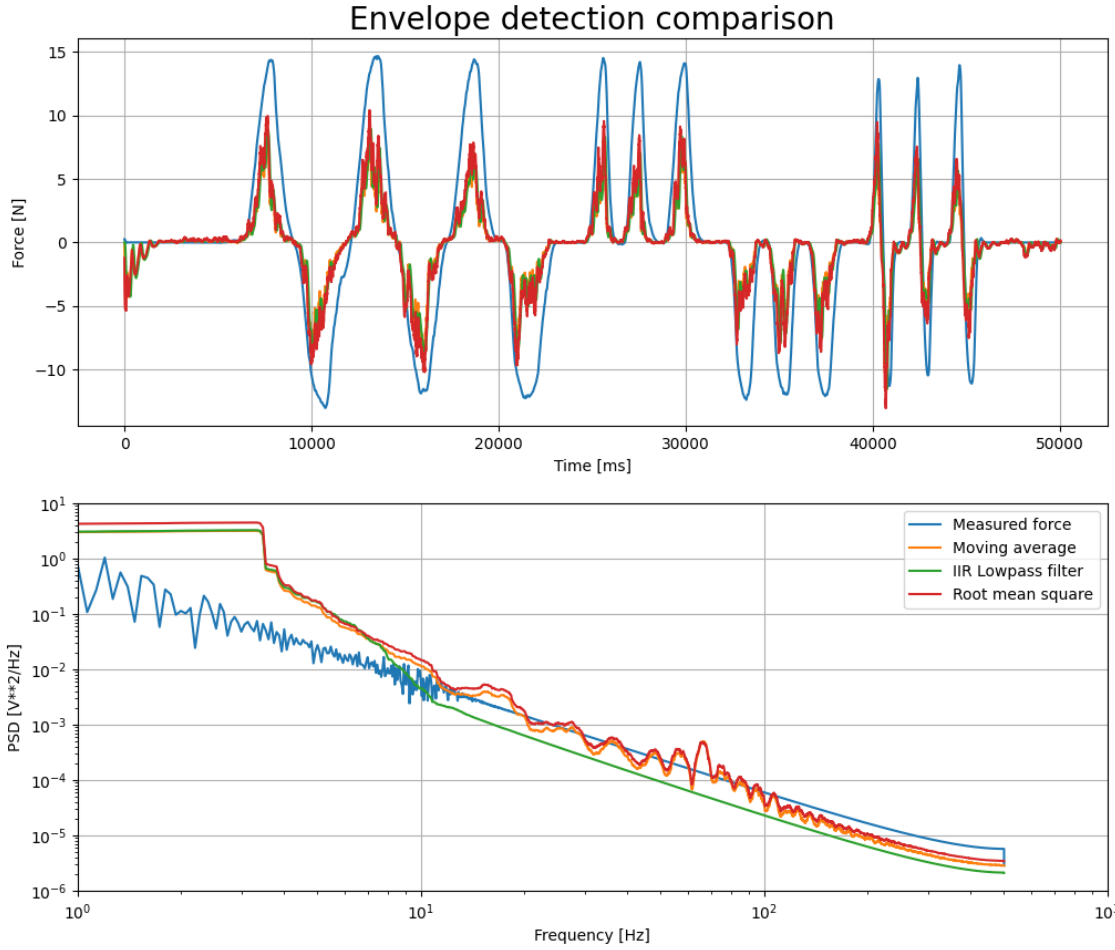

Figure 4.8: This figure illustrates the effect that different envelope estimation techniques have on sEMG signal. The signals were not whitened and not filtered. Even though all methods seem to provide almost identical behaviour in the time domain it can be seen from the frequency spectra that this only holds for moving average and root mean square envelope detection. IIR Butterworth low-pass filtering results in a more linear attenuation from the f_{cut} on wards (set to 5 Hz) which is in line with the simulations as seen in Figure 3.13

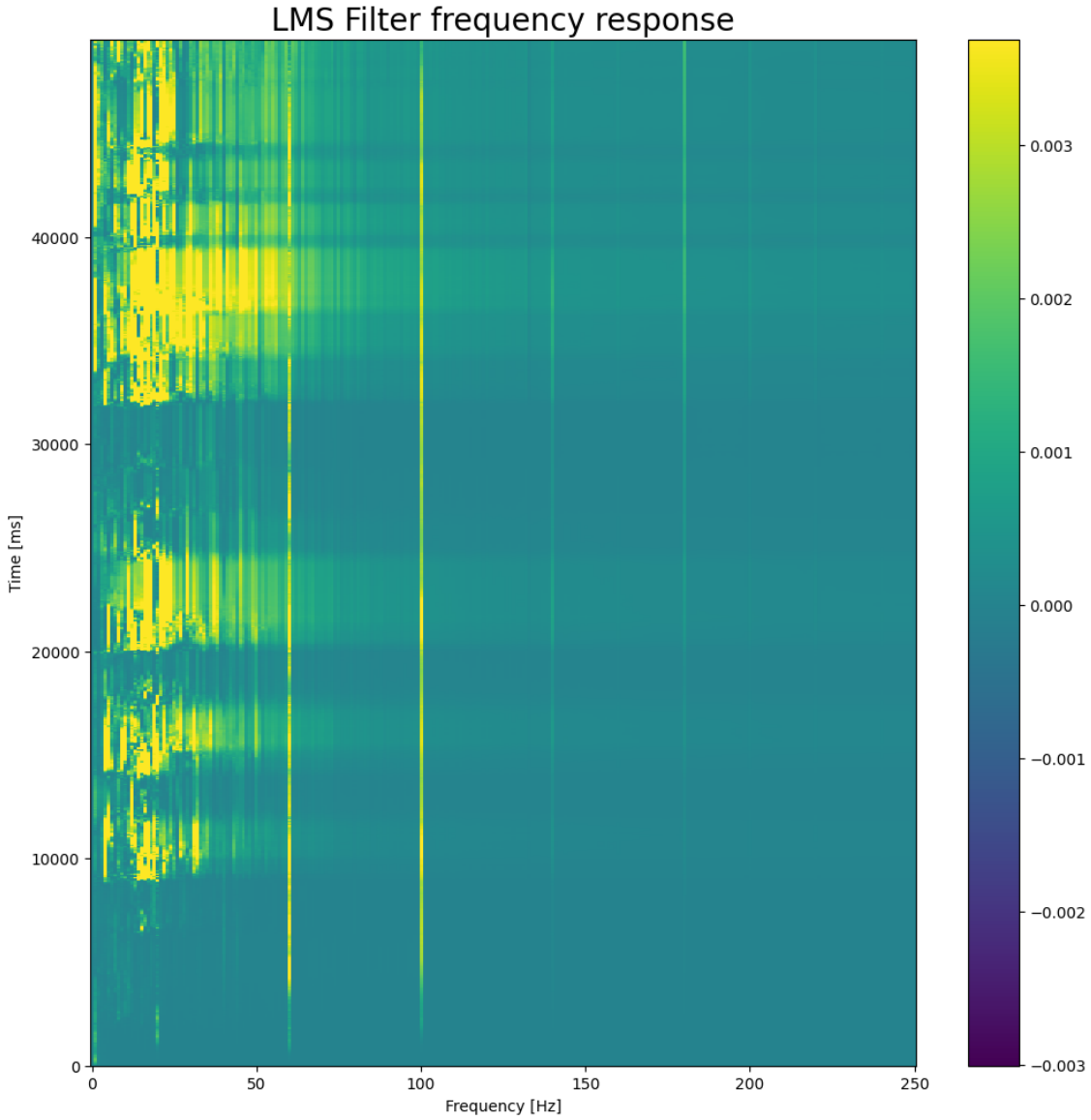

Figure 4.9: The frequency response of the adaptive LMS filter over time. It can be seen that lower frequencies are attenuated, as well as a constantly present signal around 60 Hz and one at 100 Hz. Very faintly it can also be seen that around 150 Hz and 200 Hz the frequencies are attenuated, it is expected that these are the harmonic overtones of nearby power lines.

Figure 4.9 shows the adapting frequency response of the LMS filter. Comparing this spectrogram with the raw measurements as seen in Figure 4.4 the connection can be made between muscle contractions (starting at 10 s) and the filter coefficients adjusting.

4.4 Conclusion

Figure 4.5 shows the results that allow comparing different signal processing chains. Furthermore the individual processing steps have been compared in the time and frequency domain to show any notable characteristics. Further observations are made in the Discussion section 5.1 and compared to expectations made after the simulations.

5 Discussion and conclusion

5.1 Discussion

It can be seen from the lag comparison subplot in Figure 4.5 that only signal processing chains that use whitening appear to introduce lag. This could be caused by the phase delay that is introduced by the whitening filter. If the filter were to have a linear phase then all frequencies would be equally delayed resulting in a constant group delay. If this filter did not have linear phase but instead introduces a stronger phase delay in higher frequencies, then the total delay would become more apparent when amplifying these higher frequencies [63]. The amplification of higher frequencies does happen in the whitening filter as can be seen in the simulation in 3.1, and the time domain plot shows signs of introduction of delay in the filtered signal which can stem from making higher frequencies with more phase delay more prominent. In the simulations the phase of the whitening filter was set to the phase of the input signal ('source' of filter).

A perhaps much more intriguing result stemming from the lag subplot in Figure 4.5 is the introduction of *negative lag* in some processing combinations. This indicates that some processing methods allow *predicting* when and how much force will be applied. Even though that may seem impossible at first it can actually be explained very intuitively. sEMG measures the activation of a muscle, the activation of a muscle leads to muscle contraction, and muscle contraction results in a force being applied to the arm. Since the arm has weight, this force first results in acceleration before it is transferred to the handle connected to the load cell. As a result the sEMG signal is measured slightly before the actual force is measured by the load cell. This is in line with literature [4]. Using some processing chains the force can be predicted around 500 ms before it is applied to and measured by the load cell. In terms of lag it can also be noticed that using zero phase for the whitening filter seems to reduce a large portion of the lag as can be seen in appendix Figure A.4.

One processing step that stands out in the lag plot of Figure 4.5 is adaptive filtering. It can be seen that applying an adaptive LMS filter results in unusually fast response time (negative lag) of up to 550 ms when combined with RMS envelope detection. Adaptive filtering does seem to introduce more error as seen in the error subplot, but this is marginal compared to other filtering methods.

Lastly it seems that the IIR Butterworth lowpass filter for envelope detection consistently introduces approximately 5% lag compared to moving average or RMS envelope detection. This is consistent across all filters and whitening as can be seen in the lag subplot in Figure 4.5. This is also consistent with simulations as seen in Figures 3.16 and 3.15 given the filter length and cutoff frequency that were used in the measurements.

The goal of this research was to find the best combination of whitening, filtering, and envelope detection to estimate force from sEMG.

The answer to this question depends on the application. If lag is the sole/primary concern then the processing chain of no whitening, adaptive LMS filter, and RMS envelope detection is the ideal solution as it results in the most negative lag, closely followed by moving average envelope detection. If error is the primary concern then no whitening, no filtering, and RMS envelope detection is the optimal solution.

The fact that the lowest error rates are achieved in processing chains that include no filtering hints at the fact that improving the signal to noise ratio of an sEMG signal does not necessarily result in a better estimation of the applied force. This observation can be used to construct processing chains of lower computational complexity due to the omission of a major processing

step as seen in Figure 1.1. It should be noted that this conclusion is drawn from a single measurement at a single location and thus may yield different results in different environments.

5.2 Conclusion

In this report a complete signal processing chain for sEMG signals was presented. Within each step in this processing chain various processing techniques were discussed and tested to illustrate their behaviour and performance when applied to sEMG signals.

In a simulated environment it was shown that static filter performance does not depend on MVC, and that a Wiener filter provides the highest SNR after filtering (Figure 3.9). However, this came at the cost of the worst bandwidth of all filtering techniques (Figure 3.10).

Applying filtering in a practical situation to accurately estimate force from sEMG shows that high SNR but low bandwidth does not relate to high accuracy. As a result, not applying any filtering on the sEMG signal provided the best results in terms of error. Adaptive LMS filtering *did* perform the best in terms of lag in some scenarios preceding the measured force signal by 550 ms.

The conclusion drawn from comparing different envelope estimation techniques is that infinite impulse response Butterworth lowpass filter introduces significantly more lag than moving average and RMS filtering, both of which performed approximately the same with moving average yielding a slightly better in terms of lag.

Lastly, whitening introduced significant lag across all filters and envelope detection methods.

5.3 Recommendations

One area where the results presented in this report can be improved is by using a larger data set to apply the processing techniques to. Since the techniques were only validated using a single long measurement it is very well possible that the techniques function differently in different environments or with different hardware.

Concerning the implementation of filters, it might be interesting to develop and test a more elaborate algorithm that can for example change the window size of the adaptive filter based on the amplitude of the signal. This could reduce the required processing power to implement certain processing chains. Additionally the notable results from adaptive LMS filtering in terms of lag suggests more research into optimization of this filter. Since only a single combination of filter length and convergence coefficient was used (drawn from simulated data), it might be useful to determine a wider range of variables on sEMG data sets.

This report also assumed a linear relation between the sEMG and the estimated force. Future research could possible explore different relations and the influence of different signal processing chains.

Lastly, this report has given insight into the performance of different processing techniques but has mostly omitted the computational complexity that is required to apply them in real-time such as robotic prostheses [64] which have limited processing power. Future research should be done into the capabilities of modern processing techniques to draw a conclusion on whether or not this forms an issue.

A Appendix 1

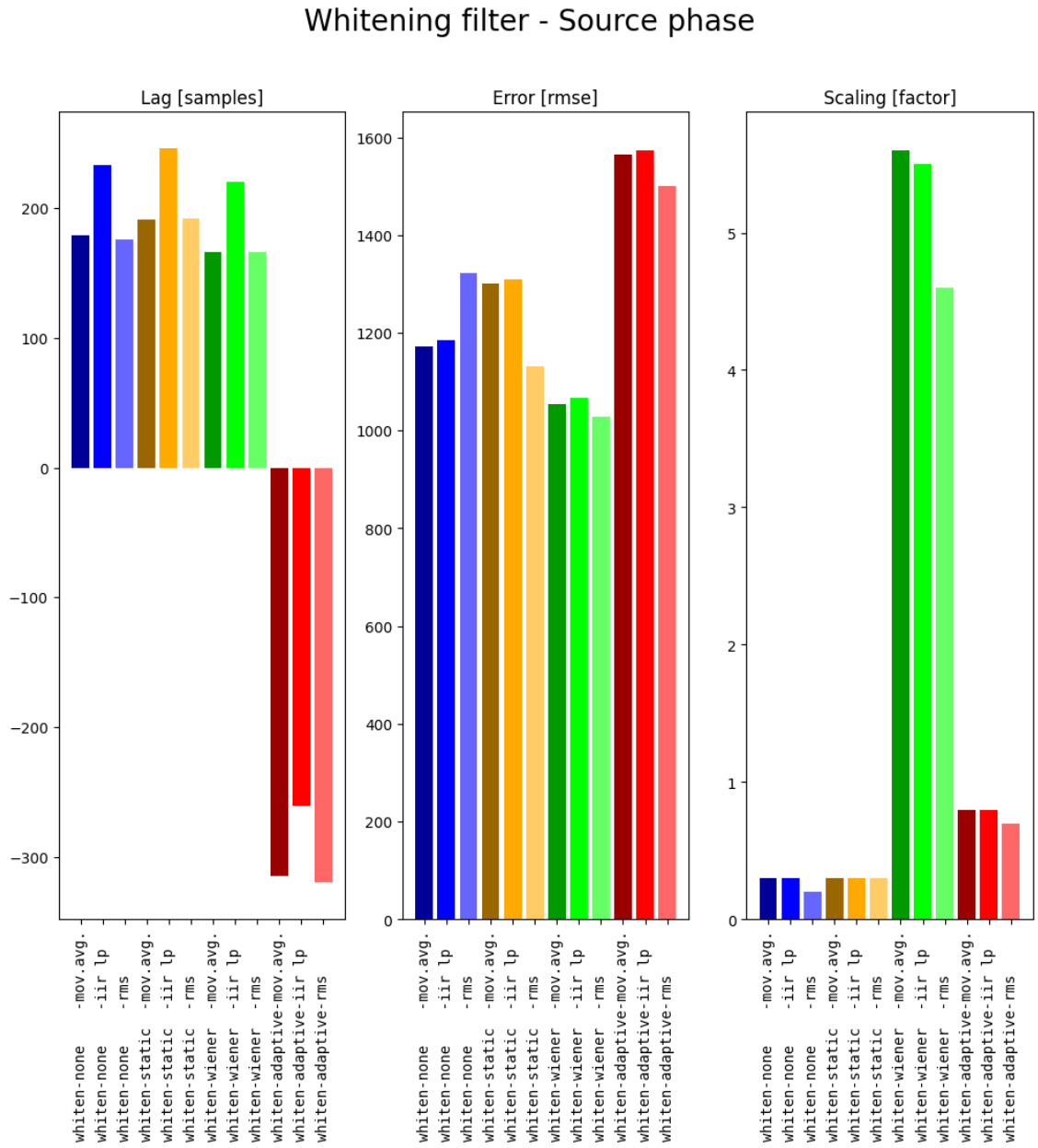

Figure A.1: Lag, error, and scaling of different filtering and envelope techniques with whitening applied. The whitening filter is constructed from the desired frequency amplitude response and a phase. The frequency response is determined as described in the simulation section 3.1, and the phase is set to the phase of the input signal that was used to construct the whitening filter.

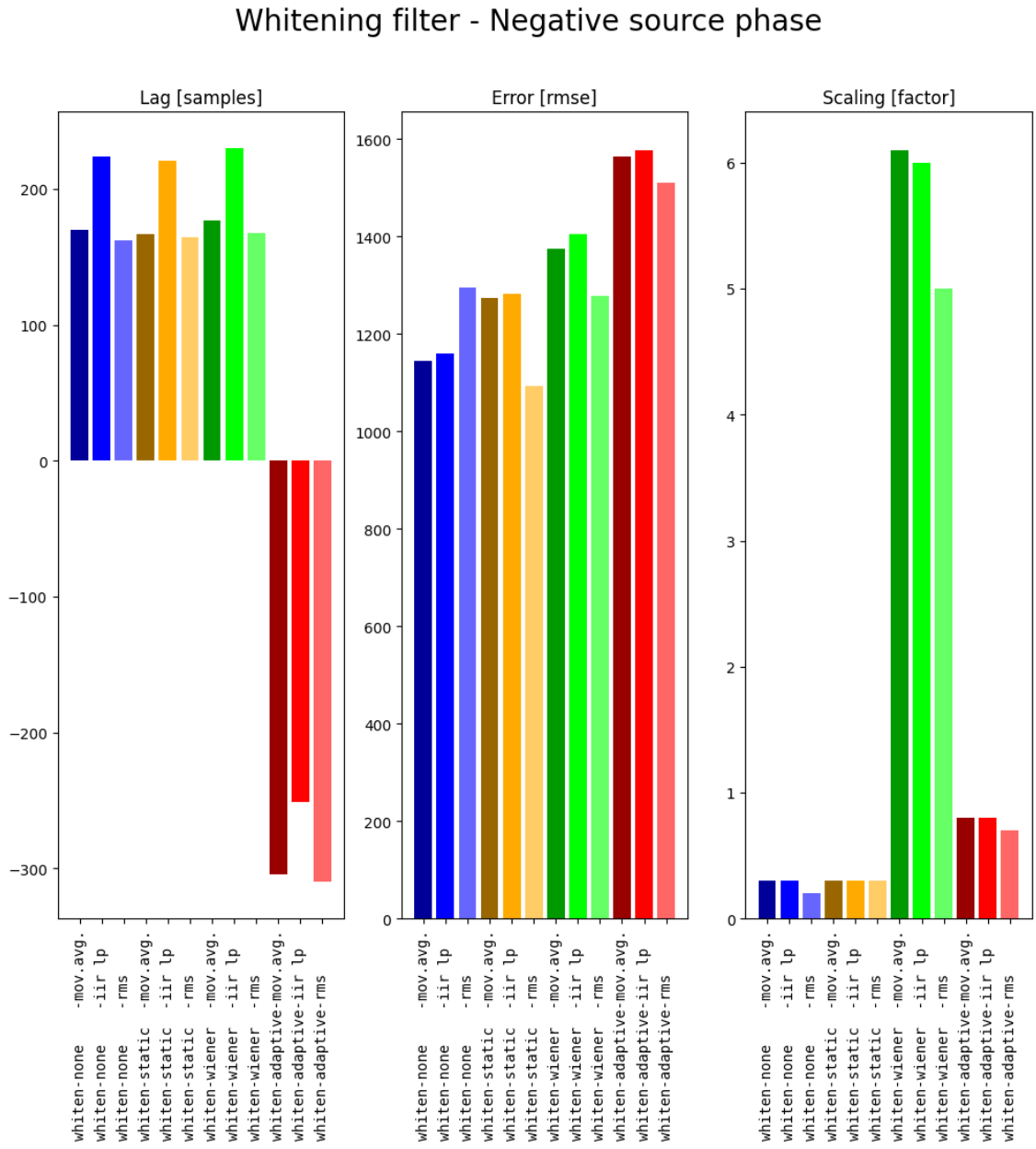

Figure A.2: Lag, error, and scaling of different filtering and envelope techniques with whitening applied. The whitening filter is constructed from the desired frequency amplitude response and a phase. The frequency response is determined as described in the simulation section 3.1, and the phase is set to the negative phase of the input signal that was used to construct the whitening filter.

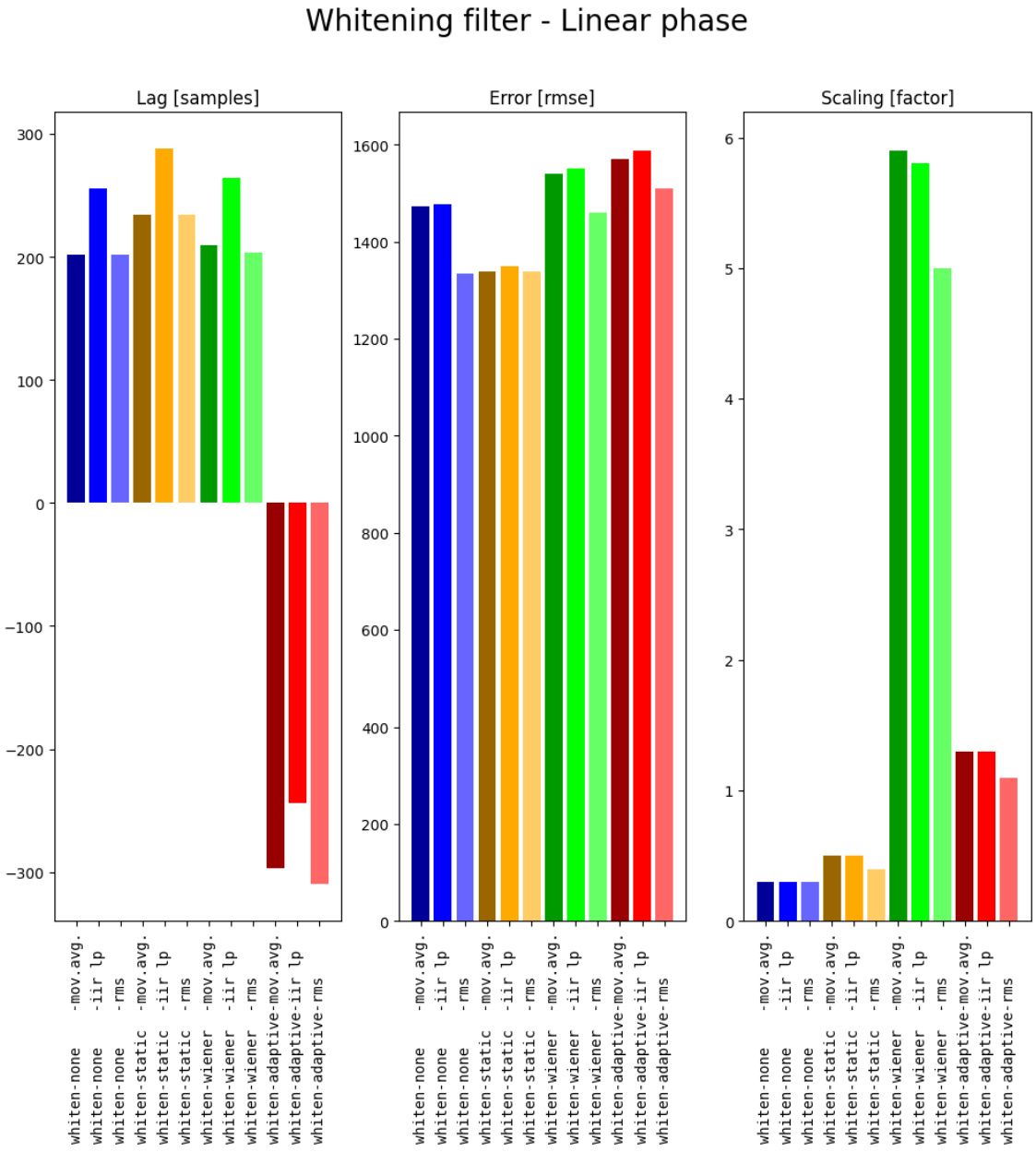

Figure A.3: Lag, error, and scaling of different filtering and envelope techniques with whitening applied. The whitening filter is constructed from the desired frequency amplitude response and a phase. The frequency response is determined as described in the simulation section 3.1, and the phase is set to linear phase.

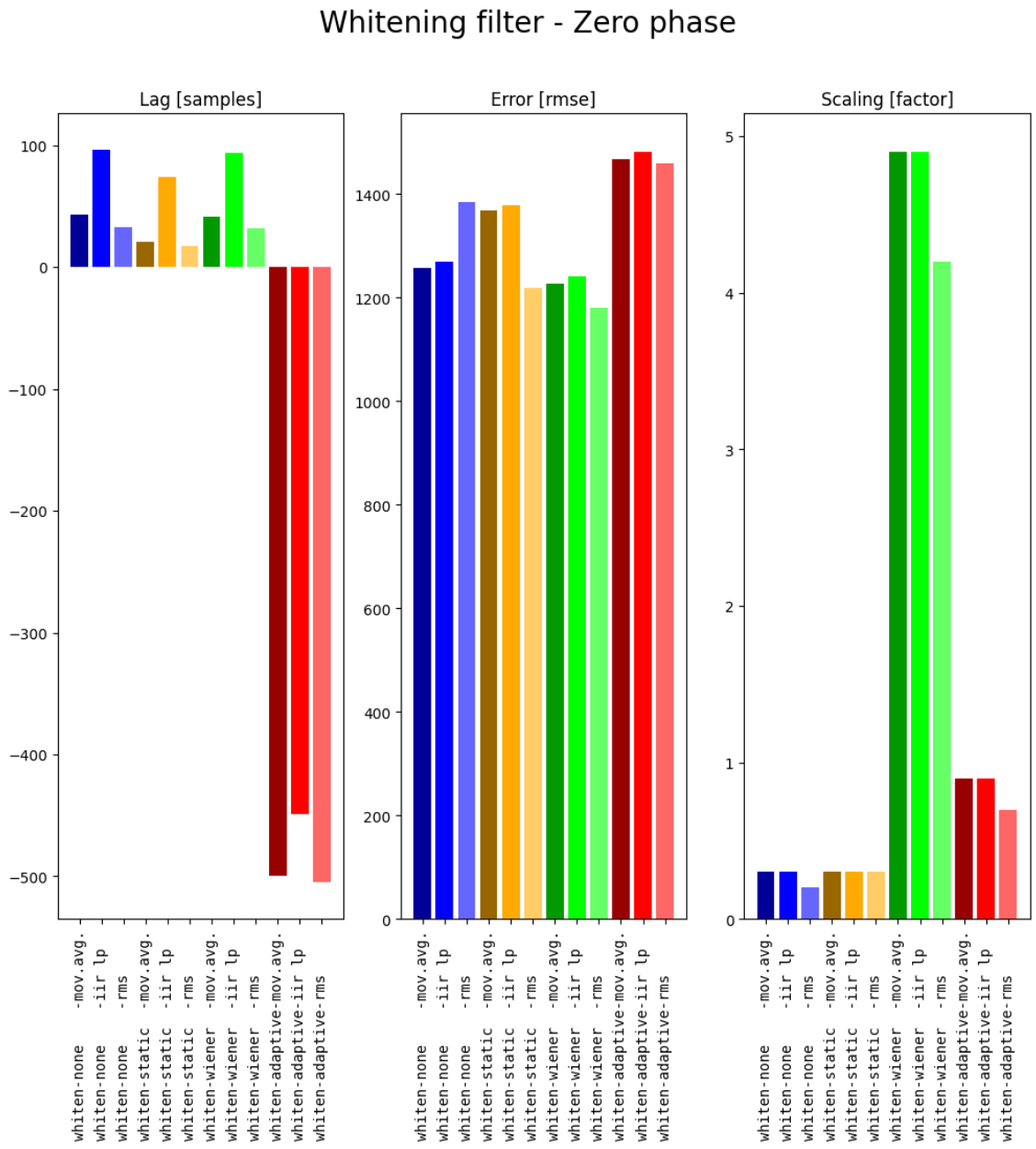

Figure A.4: Lag, error, and scaling of different filtering and envelope techniques with whitening applied. The whitening filter is constructed from the desired frequency amplitude response and a phase. The frequency response is determined as described in the simulation section 3.1, and the phase is set to zero phase.

Bibliography

[1] D. Robertson, G. Caldwell, J. Hamill, G. Kamen, and S. Whittlesey, *Research Methods in Biomechanics: Second edition (eBook)*, 11 2013.

[2] "Electromyography," Apr 2022. [Online]. Available: https://en.wikipedia.org/wiki/Electromyography

[3] J. Lobo Prat, P. Kooren, A. Stienen, J. Herder, H. Koopman, and P. Veltink, "Non-invasive control interfaces for intention detection in active movement-assistive devices," *Journal of neuroengineering and rehabilitation*, vol. 11, no. 1, pp. –, 2014.

[4] E. Burdet, D. Franklin, and T. Milner, *Human Robotics: Neuromechanics and Motor Control*, 01 2013.

[5] M. M. Janssen, J. Harlaar, and I. J. de Groot, "Surface emg to assess arm function in boys with dmd: A pilot study," *Journal of Electromyography and Kinesiology*, vol. 25, no. 2, pp. 323–328, 2015. [Online]. Available: https://www.sciencedirect.com/science/article/pii/S1050641115000279

[6] T. J. Roberts and A. M. Gabaldón, "Interpreting muscle function from EMG: lessons learned from direct measurements of muscle force," *Integr. Comp. Biol.*, vol. 48, no. 2, pp. 312–320, Aug. 2008.

[7] M. Z. Jamal, D.-H. Lee, and D. J. Hyun, "Real time adaptive filter based emg signal processing and instrumentation scheme for robust signal acquisition using dry emg electrodes," in *2019 16th International Conference on Ubiquitous Robots (UR)*, 2019, pp. 683–688.

[8] L. Smith and L. Hargrove, "Comparison of surface and intramuscular emg pattern recognition for simultaneous wrist/hand motion classification," *Conference proceedings : ... Annual International Conference of the IEEE Engineering in Medicine and Biology Society. IEEE Engineering in Medicine and Biology Society. Conference*, vol. 2013, pp. 4223–4226, 07 2013.

[9] R. Merletti and D. Farina, "Analysis of intramuscular electromyogram signals," *Philosophical transactions. Series A, Mathematical, physical, and engineering sciences*, vol. 367, pp. 357–68, 12 2008.

[10] Wikipedia, "Electromyography — Wikipedia, the free encyclopedia," http://en.wikipedia.org/w/index.php?title=Electromyography&oldid=1081392040, 2022, [Online; accessed 23-June-2022].

[11] S. Dick F., K. Bert U., L. Bernd G., and V. D. Johannes P., "High-density surface emg: Techniques and applications at a motor unit level," *Biocybernetics and Biomedical Engineering*, vol. 32, no. 3, pp. 3–27, 2012. [Online]. Available: https://www.sciencedirect.com/science/article/pii/S0208521612700396

[12] G. Drost, D. Stegeman, B. Van Engelen, and M. Zwarts, "Clinical applications of high-density surface emg: A systematic review," *Journal of electromyography and kinesiology : official journal of the International Society of Electrophysiological Kinesiology*, vol. 16, pp. 586–602, 01 2007.

[13] T. Chung, J. Q. Wang, J. Wang, B. Cao, Y. Li, and S. W. Pang, "Electrode modifications to lower electrode impedance and improve neural signal recording sensitivity," *J. Neural Eng.*, vol. 12, no. 5, p. 056018, Oct. 2015.

[14] D. Goueytes, A. Abbasi, H. Lassagne, D. E. Shulz, L. Estebanez, and V. Ego-Stengel, "Control of a robotic prosthesis simulation by a closed-loop intracortical brain-machine interface," in *2019 9th International IEEE/EMBS Conference on Neural Engineering (NER)*, 2019, pp. 183–186.

[15] M. hanine, E. Abdelmounim, R. Haddadi, and B. Abdelaziz, "Real time emg noise cancellation from ecg signals using adaptive filtering," 11 2017, pp. 1–6.

[16] S. Ranaldi, G. Corvini, C. De Marchis, and S. Conforto, "The influence of the semg amplitude estimation technique on the emg–force relationship," *Sensors*, vol. 22, no. 11, 2022. [Online]. Available: https://www.mdpi.com/1424-8220/22/11/3972

[17] G. Yadav, B. Krishna, and M. Kamaraju, "Performance of wiener filter and adaptive filter for noise cancellation in real-time environment," *International Journal of Computer Applications*, vol. 97, 07 2014.

[18] J. Liu, D. Ying, and P. Zhou, "Wiener filtering of surface EMG with a priori SNR estimation toward myoelectric control for neurological injury patients," *Med Eng Phys*, vol. 36, no. 12, pp. 1711–1715, Oct. 2014.

[19] L. Liu, p. Liu, E. Clancy, E. Scheme, and K. Englehart, "Electromyogram whitening for improved classification accuracy in upper limb prosthesis control," *IEEE transactions on neural systems and rehabilitation engineering : a publication of the IEEE Engineering in Medicine and Biology Society*, vol. 21, 03 2013.

[20] E. Clancy and K. Farry, "Adaptive whitening of the electromyogram to improve amplitude estimation," *IEEE transactions on bio-medical engineering*, vol. 47, pp. 709–19, 07 2000.

[21] N. Hogan and R. W. Mann, "Myoelectric signal processing: Optimal estimation applied to electromyography - part i: Derivation of the optimal myoprocessor," *IEEE Transactions on Biomedical Engineering*, vol. BME-27, no. 7, pp. 382–395, 1980.

[22] S. N. Omar, "Application of digital signal processing and machine learning for electromyography: A review," *Asian Journal Of Medical Technology*, vol. 1, pp. 30–45, 07 2021.

[23] Y. Zhou, R. Chen, M. Cheng, Y. Alshahrani, S. Franovic, E. Lau, G. Xu, G. Ni, J. Cavanaugh, S. Muh, and S. Lemos, "Comparison of machine learning methods in semg signal processing for shoulder motion recognition," *Biomedical Signal Processing and Control*, vol. 68, p. 102577, 07 2021.

[24] "Reliable machine learning," Jan 2022. [Online]. Available: https://www.microsoft.com/en-us/research/group/reliable-machine-learning/

[25] D. U. Silverthorn, B. R. Johnson, W. C. Ober, and C. W. Ober, *Human physiology: An integrated approach*. Pearson Education, Inc., 2016.

[26] E. N. Marieb and K. Hoehn, *9 - Skeletal Muscle*. Pearson Benjamin Cummings, 2007.

[27] G. Wolterink, R. Sanders, F. Muijzer, B.-J. van Beijnum, and G. Krijnen, "3d-printing soft semg sensing structures," in *2017 IEEE SENSORS*, 2017, pp. 1–3.

[28] S. Haykin and M. Moher, *An Introduction to Analog and Digital Communications*. Wiley, 2007. [Online]. Available: https://books.google.nl/books?id=ovLztgEACAAJ

[29] B. P. Lathi, *Chapter 3 - Time-domain analysis of discrete-time systems*. Oxford University Press, 2010.

[30] Inductiveload. (2009) A general finite impulse response filter with n stages, each with an independent delay, di, and amplification gain, ai. [Online]. Available: https://upload.wikimedia.org/wikipedia/commons/0/07/FIR_Filter_General.svg

[31] Wikipedia, "Wiener filter — Wikipedia, the free encyclopedia," http://en.wikipedia.org/w/index.php?title=Wiener%20filter&oldid=1093059630, 2022, [Online; accessed 29-June-2022].

[32] C. Z. Siavash Safapourhajari, Andrés Alayón Glazunov, "Lecture - adaptive filters 1," 2022.

[33] L.-M. Dogariu, J. Benesty, C. Paleologu, and S. Ciochină, "An insightful overview of the wiener filter for system identification," *Applied Sciences*, vol. 11, no. 17, 2021. [Online]. Available: https://www.mdpi.com/2076-3417/11/17/7774

[34] "Ee264: Lecture 12 - wiener filtering." [Online]. Available: https://web.stanford.edu/class/archive/ee/ee264/ee264.1072/mylecture12.pdf

[35] "Probability course - stationary process." [Online]. Available: https://www.probabilitycourse.com/chapter10/10_1_4_stationary_processes.php

[36] A. the Editorial StaffEditorial Staff at Ask Any Difference is a team of experts in the field of "Difference Between" topics and led by Sandeep Bhandari, "Difference between stationary and non-stationary signals," Jan 2022. [Online]. Available: https://askanydifference.com/difference-between-stationary-and-non-stationary-signals/

[37] S. J. Orfanidis, *Chapter 7.3 - The Widrow-Hoff LMS Adaptation Algorithm*. Sophocles J. Orfanidis, 2007.

[38] L. Tan and J. Jiang, "Chapter 9 - adaptive filters and applications," in *Digital Signal Processing (Third Edition)*, third edition ed., L. Tan and J. Jiang, Eds. Academic Press, 2019, pp. 421–474. [Online]. Available: https://www.sciencedirect.com/science/article/pii/B9780128150719000099

[39] C. Z. Siavash Safapourhajari, Andrés Alayón Glazunov, "Lecture - adaptive filters 2," 2022.

[40] S. S. Haykin, *Chapter 9.11 - Normalized LMS Algorithm*. Prentice Hall, 1996.

[41] A. K. says:, C. H. says:, A. A. N. W. says:, and C. says:, "Active noise cancellation using the wiener filter," Jun 2019. [Online]. Available: https://grittyengineer.com/noise-cancellation-using-the-wiener-filter/

[42] Admin, "Difference between iir and fir filters: A practical design guide," Nov 2021. [Online]. Available: https://www.advsolned.com/difference-between-iir-and-fir-filters-a-practical-design-guide/

[43] V. MADISETTI, *The Digital Signal Processing Handbook*, ser. Electrical Engineering Handbook. Taylor & Francis, 1997. [Online]. Available: https://books.google.nl/books?id=Zhc36gyobk0C

[44] Mathuranathan, "Choosing fir or iir ? understand design perspective," May 2021. [Online]. Available: https://www.gaussianwaves.com/2017/02/choosing-a-filter-fir-or-iir-understanding-the-design-perspective/

[45] E. Clancy and N. Hogan, "Single site electromyograph amplitude estimation," *IEEE Transactions on Biomedical Engineering*, vol. 41, no. 2, pp. 159–167, 1994.

[46] C. E. Shannon, "A mathematical theory of communication," *The Bell System Technical Journal*, vol. 27, pp. 379–423, 1948. [Online]. Available: http://plan9.bell-labs.com/cm/ms/what/shannonday/shannon1948.pdf

[47] R. E. Thomson and W. J. Emery, "Chapter 5 - time series analysis methods," in *Data Analysis Methods in Physical Oceanography (Third Edition)*, third edition ed., R. E. Thomson and W. J. Emery, Eds. Boston: Elsevier, 2014, pp. 425–591. [Online]. Available: https://www.sciencedirect.com/science/article/pii/B9780123877826000053

[48] C. Banton, "Serial correlation definition," Feb 2022. [Online]. Available: https://www.investopedia.com/terms/s/serial-correlation.asp

[49] a. t. S. b. A. D. original work by User:Omegatron. A signal in blue and the magnitude of its analytic signal in red, showing the envelope effect.

[50] A. Goen and D. Tiwari, "Review of surface electromyogram signals: Its analysis and applications," *International Journal of Electrical, Computer, Energetic, Electronic and Communication Engineering*, vol. 7, pp. 1429–1437, 01 2013.

[51] "Digital envelope detection: The good, the bad, and the ugly." [Online]. Available: https://www.dsprelated.com/showarticle/938.php

[52] Webmaster, "Fir filter properties," Mar 2017. [Online]. Available: https://dspguru.com/dsp/faqs/fir/properties/

[53] S. W. Smith, "Chapter 15 - moving average filters," in *Digital Signal Processing*, S. W. Smith, Ed. Boston: Newnes, 2003, pp. 277–284. [Online]. Available: https://www.sciencedirect.com/science/article/pii/B9780750674447500522

[54] W. Rose, "Electromyogram analysis," *Online course material. University of Delaware. Retrieved July*, vol. 5, p. 2016, 2011.

[55] "The statistical nature of noise analysis: An introduction - technical articles." [Online]. Available: https://www.allaboutcircuits.com/technical-articles/introduction-to-statistical-noise-analysis-basic-calculations/

[56] C. Mokri, M. Bamdad, and V. Abolghasemi, "Muscle force estimation from lower limb emg signals using novel optimised machine learning techniques," *Medical & Biological Engineering & Computing*, vol. 60, no. 3, pp. 683–699, Mar 2022. [Online]. Available: https://doi.org/10.1007/s11517-021-02466-z

[57] D. Heeger, "Linear systems theory." [Online]. Available: https://www.cns.nyu.edu/~david/handouts/linear-systems/linear-systems.html

[58] D. Herres, "Bandwidth basics and fundamentals." [Online]. Available: https://www.testandmeasurementtips.com/bandwidth-basics-and-fundamentals/

[59] Wikipedia, "Cross-correlation — Wikipedia, the free encyclopedia," http://en.wikipedia.org/w/index.php?title=Cross-correlation&oldid=1083801732, 2022, [Online; accessed 26-June-2022].

[60] TMSi, "Unipolar vs. bipolar eeg measurement." [Online]. Available: https://info.tmsi.com/blog/measurement-principles#:~:text=In%20a%20bipolar%20measurement%2C%20the,against%20one%20so%20called%20reference.

[61] D. Stegeman and H. Hermens, "Standards for suface electromyography: The european project surface emg for non-invasive assessment of muscles (seniam)," vol. 1, 01 2007.

[62] D. Related, "Transient response, steady state, and decay: Introduction to digital filters." [Online]. Available: https://www.dsprelated.com/freebooks/filters/Transient_Response_Steady_State.html

[63] R. Lacoste, "Group delay basics - more filter fun," Jan 2021. [Online]. Available: https://circuitcellar.com/research-design-hub/group-delay-basics-more-filter-fun/

[64] W. Li, P. Shi, and H. Yu, "Gesture recognition using surface electromyography and deep learning for prostheses hand: State-of-the-art, challenges, and future," *Frontiers in Neuroscience*, vol. 15, 2021. [Online]. Available: https://www.frontiersin.org/article/10.3389/fnins.2021.621885